EcoDep 2023
Introduction to univariate time series analysis for climate data

Federico Maddanu [1]
CY University

January 9, 2023

[1] Address for Correspondence: AGM Laboratory, Cergy University, Av. Adolphe Chauvin 95302 CERGY-PONTOISE, France. Email: federico.maddanu@gmail.com.

Presentation of the course

1. Basic introduction to univariate time series model, weak stationarity, autocorrelation function, spectral density, non stationarity and long memory.
2. Decomposition of a time series in the singular components of trend, cycle and noise.
3. Implementation of the previous notions via the free software GNU-Octave, downloadable at `https://octave.org/`, which uses the typical MATLAB syntax. The CodeEcoDep.zip folder contains the OCTAVE code used to realize this course.
4. Applications on real world climate time series.

Main References and Books

1. **[Ber94]** Beran, J. (1994). Statistics for Long Memory Processes Monographs on Statistics and Applied Probability. Chapman & Hall, New York.
2. **[BD91]** Brockwell, P. J., and Davis, R. A. (1991). Time series: theory and methods: theory and methods. Springer Science & Business Media.
3. **[Has19]** Hassler, U. (2019). Time Series Analysis with Long Memory in View. Wiley, New York.
4. **[PW93]** Percival, D.B., Walden, A.T. (1993). Spectral Analysis for Physical Applications. Cambridge University Press, Cambridge.

Basic Concepts and descriptive analysis

- The main object of our analysis is the univariate time series y_t with $t = 1, \cdots, n$.
- The information set $\mathcal{I}_t$ is the series itself and its position in time, $\mathcal{I}_t = \{y_t, y_{t-1}, y_{t-2}, \cdots, y_1\}$.
- The main descriptive tool is the plot of the series, by which we represent the pair of values (t, y_t) on a Cartesian plane, which can immediately reveal the presence of important features, such as trend and cycle.

Climate time series: examples

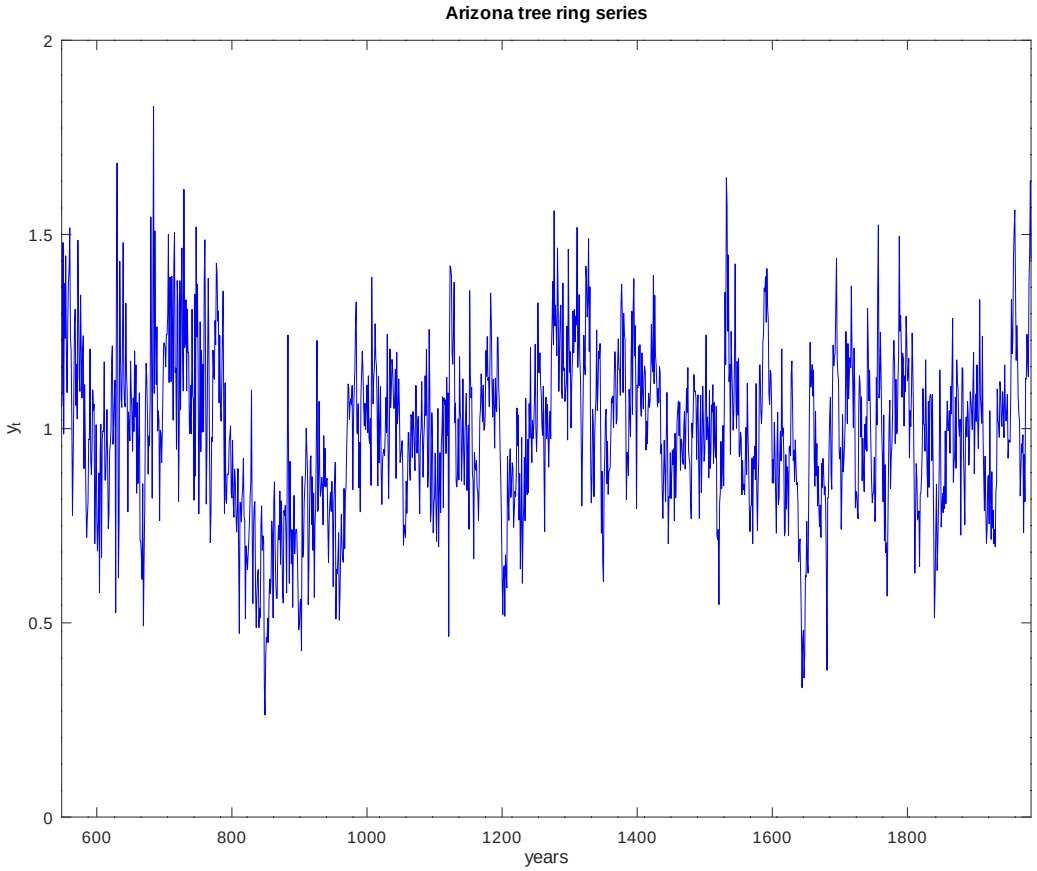

Figure: Arizona pine tree rings yearly time series.

Climate time series: examples

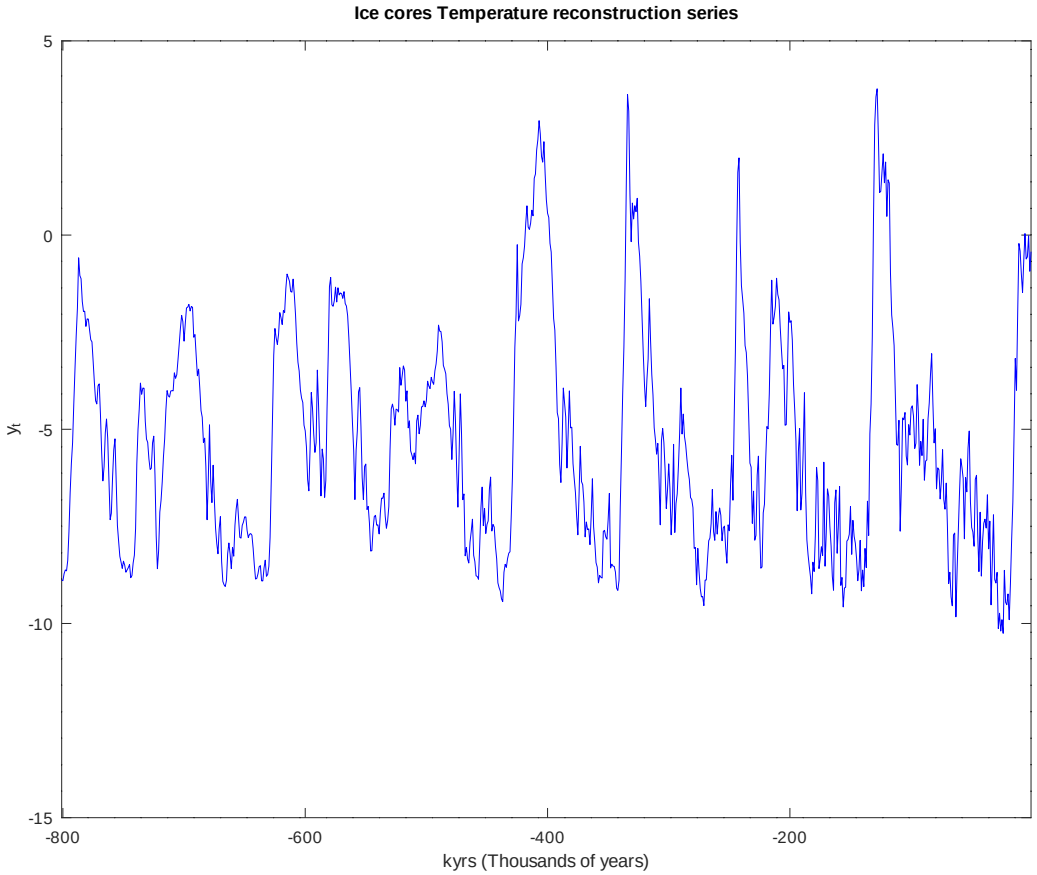

Figure: Temperature reconstruction obtained from the ice cores records collected at the South pole station EPICA Dome C.

Climate time series: examples

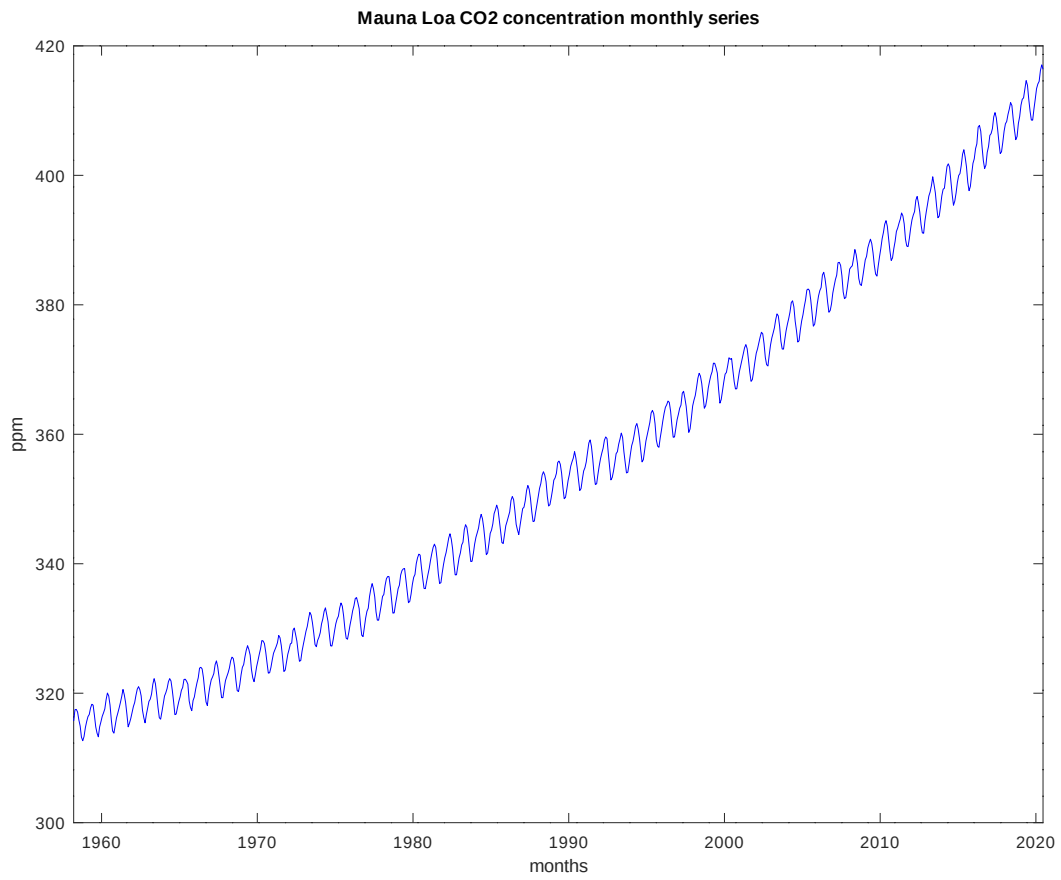

Figure: CO2 concentration ppm recorded at the observatory of Mauna Loa (Hawaii).

Stationary stochastic processes

- **Stochastic process**: a collection of random variables $(y_t(\omega); \omega \in \Omega; t \in \mathbb{Z})$ defined on a probability space $(\Omega; \mathcal{F}; P)$, where the integer number t is a time-index, Ω is the sample space, $\mathcal{F}$ is a sigma algebra defined on Ω and P is a probability measure on Ω. A time series is a realization of the stochastic process for a given $\omega \in \Omega$ and $t = 1, 2, \cdots, n$.
- **Stationarity**: y_t is weakly stationary (second order stationary) if $\forall t, k \in \mathbb{Z}$:

$$\begin{aligned} E(y_t) &= \mu \quad , \quad \mu < \infty \\ E(y_t - \mu)(y_{t-k} - \mu) &= \gamma(k) \quad , \gamma(k) < \infty \end{aligned} \tag{1}$$

Stationary stochastic processes

- $\gamma(k)$ is defined as the **Autocovariance function** (ACF) of the process y_t with $\gamma(k) = \gamma(-k)$.
- The **Spectral density** of the process y_t is defined as the discrete Fourier transform of the ACF:
  $f(\omega) = \frac{1}{2\pi} \sum_{k=-\infty}^{\infty} \gamma(k) e^{-\imath k \omega}$ with $\omega \in [-\pi, \pi]$,
  $f(\omega) = f(-\omega)$ and $f(\omega) \geq 0$.
- $g(k) = E\{[y_t - E(y_t|w_t)][y_{t-k} - E(y_{t-k}|w_t]\}$ is the **Partial Autocovariance function** (PACF) defined as the covariance between y_t and y_{t-k} having removed the effect $w_t = (y_{t-1}, y_{t-2}, \cdots, y_{t-k+1})$.
- $\rho(k) = \gamma(k)/\gamma(0)$ is defined as the **Autocorrelation function** and $-1 \leq \rho(k) \leq 1$.
- Similarly, the **Partial Autocorrelation function** follows as $g(k)/\sqrt{E\{[y_t - E(y_t|w_t)]^2 [y_{t-k} - E(y_{t-k}|w_t]^2\}}$.

Standard non-parametric estimators

- **Sample mean**: $\hat{\mu} = \frac{1}{n}\sum_{t=1}^{n} y_t$
- **Sample Variance**: $\hat{\gamma}(0) = \frac{1}{n}\sum_{t=1}^{n}(y_t - \hat{\mu})^2$
- **Sample ACF**: $\hat{\gamma}(k) = \frac{1}{n}\sum_{t=1}^{n-k}(y_t - \hat{\mu})(y_{t+k} - \hat{\mu})$
- **Periodogram**: Inconsistent but asymptotically unbiased estimator of the spectral density obtained from the discrete Fourier transform of the sample ACF:

$$I(\omega) = \frac{1}{2\pi n}\sum_{t=0}^{n-1} |(y_t - \hat{\mu})e^{-\imath\omega t}|^2 \tag{2}$$

(see Chapter 6, [PW93]).

Climate time series: examples

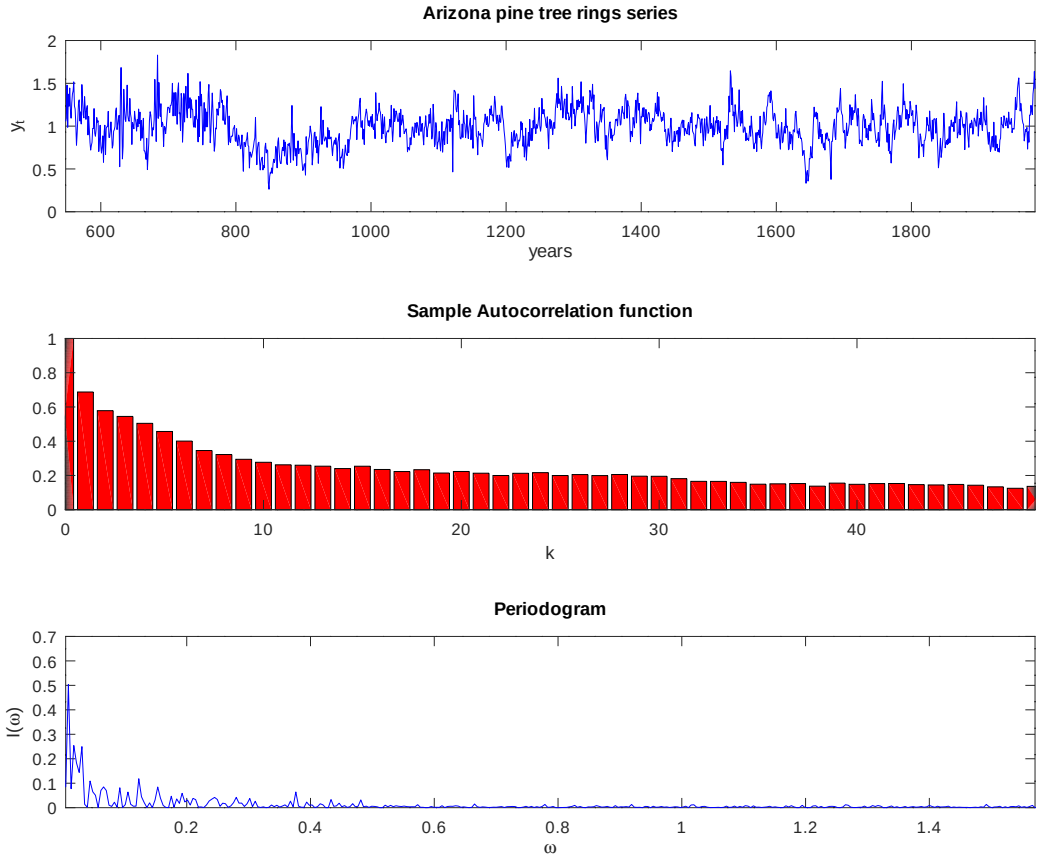

Figure: Arizona pine tree rings yearly records: time series plot, correlogram and periodogram.

Climate time series: examples

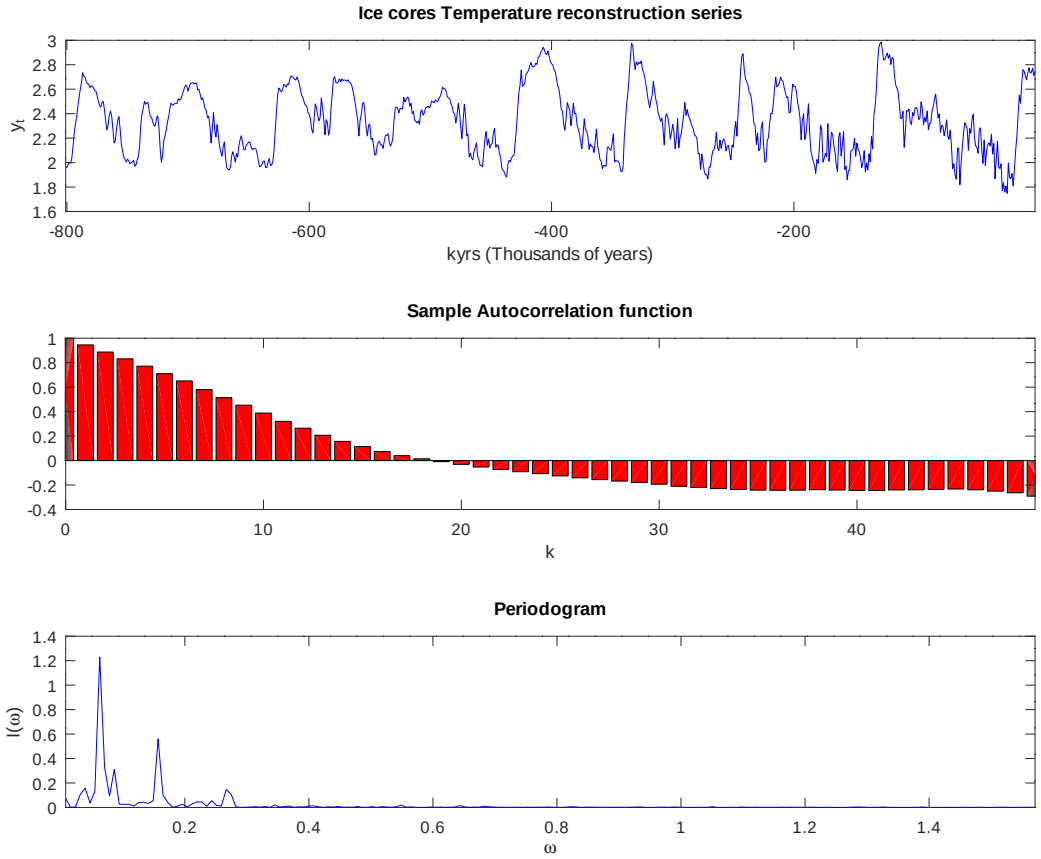

Figure: Temperature reconstruction obtained from the ice cores records collected at the South pole station EPICA Dome C: time series plot, correlogram and periodogram.

Stationary stochastic processes: linear processes

- **White noise process**: $\varepsilon_t \sim WN(0, \sigma^2)$ if

$$\begin{aligned} E(\varepsilon_t) &= 0 & \forall t \\ E(\varepsilon_t^2) &= \sigma^2 < \infty & \forall t \\ E(\varepsilon_t \varepsilon_{t-k}) &= 0 & \forall t, k \end{aligned} \tag{3}$$

  such that the spectral density is $f(\omega) = \sigma^2/2\pi$

- **Linear process**: According to the Wold decomposition, any weakly stationary process y_t can be represented by an **infinite Moving Average** process (MA(∞)) plus a deterministic component (Th. 5.7.1, [BD91]):

$$y_t = \mu + \varepsilon_t + \psi_1 \varepsilon_{t-1} + \psi_2 \varepsilon_{t-2} + \cdots = \mu + \psi(L)\varepsilon_t \tag{4}$$

  where $\psi(L) = \sum_{j=0}^{\infty} \psi_j L^j$, with $\psi_0 = 1$ and $L^j y_t = y_{t-j}$. Because of stationarity we have $\sum_{j=0}^{\infty} \psi_j^2 < \infty$ (square summability) and $E(y_t) = \mu$, while $\gamma(k) = \sigma^2 \sum_{j=0}^{\infty} \psi_j \psi_{j+k}$.

Stationary stochastic processes: The power transfer function

- The spectral density of a weakly stationary process can be computed via the **power transfer function** which maps the polynomial $\psi(z) = \psi_0 + \psi_1 z + \psi_2 z^2 + \cdots$ from the time domain to the frequency domain:

$$\psi(z) \longmapsto \psi(e^{-\imath\omega}) \tag{5}$$

  where $\psi(e^{-\imath\omega}) = \psi_0 + \psi_1 e^{-\imath\omega} + \psi_2 e^{-\imath 2\omega} + \cdots$, such that the spectral density of $y_t = \psi(L)\varepsilon_t$ is $f(\omega) = |\psi(e^{-\imath\omega})|^2 f_\varepsilon(\omega)$ where $f_\varepsilon(\omega) = \sigma^2/2\pi$ (see Chapter 4, [BD91]).
- **Example**: Consider the MA(1) process $y_t = \varepsilon_t + \psi\varepsilon_{t-1}$ where $\psi(L) = 1 + \psi L$, so
  $f(\omega) = |1 + \psi e^{-\imath\omega}|^2 \frac{\sigma^2}{2\pi} = |1 + \psi\cos(\omega) - \imath\psi\sin(\omega)|^2 \frac{\sigma^2}{2\pi} =$

$$= [\sqrt{1 + \psi^2\cos^2(\omega) + 2\psi\cos(\omega) + \psi^2\sin^2(\omega)}]^2 \frac{\sigma^2}{2\pi} =$$

$$= (1 + 2\psi\cos(\omega) + \psi^2)\frac{\sigma^2}{2\pi}$$

Stationary stochastic processes: MA processes

- **Finite Moving Average process**: $y_t \sim MA(q)$

$$y_t = \varepsilon_t + \sum_{j=1}^{q} \psi_j \varepsilon_{t-j} = \psi(L)\varepsilon_t \tag{6}$$

  with $\psi(L) = \sum_{j=0}^{q} \psi_j L^j$, $E(y_t) = 0$ and $\gamma(k) = \sigma^2 \sum_{j=0}^{q-k} \psi_j \psi_{j+k}$ if $k \leq q$ and $\gamma(k) = 0$ otherwise, while $f(\omega) = \frac{\sigma^2}{2\pi} |\psi(e^{-\imath\omega})|^2$.
- If the roots of $\psi(z)$ lies outside the unit circle, the process y_t is invertible (Th. 3.1.2, [BD91]) with infinite Autoregressive AR(∞) representation $\phi(L)y_t = \varepsilon_t$, where $\phi(L) = \psi(L)^{-1} = \sum_{j=0}^{\infty} \phi_j L^j$ and the coefficients ϕ_j follow from the convolution:

$$(\phi_0 + \phi_1 z + \phi_2 z^2 + \cdots) \cdot (\psi_0 + \psi_1 z + \cdots + \psi_q z^q) = 1 \tag{7}$$

Stationary stochastic processes: AR processes

- **Finite Autoregressive process**: $y_t \sim AR(p)$

$$y_t - \sum_{j=1}^{p} \phi_j y_{t-j} = \phi(L) y_t = \varepsilon_t \tag{8}$$

with $\phi(L) = 1 - \sum_{j=1}^{p} \phi_j L^j$ and $f(\omega) = \frac{\sigma^2}{2\pi} |\phi(e^{-\imath\omega})^{-1}|^2$.

- If the roots of $\phi(z)$ lies outside the unit circle, the process y_t is causal (Th. 3.1.1, [BD91]) with MA(∞) representation $y_t = \psi(L)\varepsilon_t$, where $\psi(L) = \phi(L)^{-1} = \sum_{j=0}^{\infty} \psi_j L^j$ and the coefficients ψ_j follow from the convolution:

$$(\psi_0 + \psi_1 z + \psi_2 z^2 + \cdots) \cdot (\phi_0 + \phi_1 z + \cdots + \phi_p z^p) = 1 \tag{9}$$

Stationary stochastic processes: AR processes

- The ACF can be computed according to

$$\begin{aligned}
\gamma(0) &= \phi_1\gamma(1) + \phi_2\gamma(2) + \cdots + \phi_p\gamma(p) + \sigma^2 \\
\gamma(1) &= \phi_1\gamma(0) + \phi_2\gamma(1) + \cdots + \phi_p\gamma(p-1) \\
&\vdots
\end{aligned}$$

such that

$$\gamma(k) = \phi_1\gamma(k-1) + \phi_2\gamma(k-2) + \cdots + \phi_p\gamma(k-p)$$

if $0 < k \leq p$ and $\gamma(k) = 0$ otherwise.

Stationary stochastic processes: The Yule-Walker equation

- The previous system of equation leads the **Yule-Walker** equation $\boldsymbol{\Gamma}_y \boldsymbol{\phi} = \boldsymbol{\gamma}_p$:

$$\begin{bmatrix} \gamma(0) & \gamma(1) & \cdots & \gamma(p-1) \\ \gamma(1) & \gamma(0) & \ddots & \gamma(p-2) \\ \vdots & \gamma(1) & \ddots & \vdots \\ \gamma(p-1) & \cdots & & \gamma(0) \end{bmatrix} \begin{bmatrix} \phi_1 \\ \phi_2 \\ \vdots \\ \phi_p \end{bmatrix} = \begin{bmatrix} \gamma(1) \\ \gamma(2) \\ \vdots \\ \gamma(p) \end{bmatrix} \tag{10}$$

where $\boldsymbol{\Gamma}_y = E([y_1, y_2, \cdots, y_n][y_1, y_2, \cdots, y_n]')$ is the covariance matrix of y_t.

Stationary stochastic processes: The DL algorithm

- For $m = 2, \cdots, p$ and initialising $\hat{\phi}_1 = \frac{\hat{\gamma}(1)}{\hat{\gamma}(0)}$ and $\hat{\nu}_1 = \hat{\gamma}(0)\left(1 - \frac{\hat{\gamma}(1)^2}{\hat{\gamma}(0)^2}\right)$, $\hat{\boldsymbol{\phi}}_p$ can be computed recursively via the Durbin Levinson (DL) algorithm (Prop. 8.2.1, [BD91]):

$$\hat{\phi}_{m,m} = \left(\hat{\gamma}(m) - \begin{bmatrix} \hat{\phi}_{m-1,1} & \cdots & \hat{\phi}_{m-1,m-1} \end{bmatrix} \begin{bmatrix} \hat{\gamma}(m-1) \\ \vdots \\ \hat{\gamma}(1) \end{bmatrix}\right) \hat{\nu}_{m-1}^{-1}$$

$$\begin{bmatrix} \hat{\phi}_{m,1} \\ \vdots \\ \hat{\phi}_{m,m-1} \end{bmatrix} = \begin{bmatrix} \hat{\phi}_{m-1,1} \\ \vdots \\ \hat{\phi}_{m-1,m-1} \end{bmatrix} - \hat{\phi}_{m,m} \begin{bmatrix} \hat{\phi}_{m-1,m-1} \\ \vdots \\ \hat{\phi}_{m-1,1} \end{bmatrix}$$

$$\hat{\nu}_m = \hat{\nu}_{m-1}(1 - \hat{\phi}_{m,m}^2)$$

where $\hat{\phi}_{m,m}$ are the partial autocorrelations, $\hat{\gamma}(k)$ is the estimated ACF and ν_n is the one-step-ahead mean square prediction error.

Stationary stochastic processes: The DL algorithm

Through the DL algorithm, we can estimate the inverse covariance matrix via the following decomposition:

$$\hat{\mathbf{\Gamma}}_p^{-1} = \hat{\mathbf{C}}_p' \hat{\mathbf{D}}_p \hat{\mathbf{C}}_p \tag{11}$$

where $\hat{\mathbf{D}}_p = \text{diag}(\hat{\nu}_0^{-1}, \hat{\nu}_1^{-1}, \cdots, \hat{\nu}_{p-1}^{-1})$ with $\hat{\nu}_0 = \hat{\gamma}(0)$ and:

$$\hat{\mathbf{C}}_p = \begin{bmatrix} 1 & 0 & 0 & \cdots & 0 \\ -\hat{\phi}_{1,1} & 1 & 0 & \cdots & 0 \\ -\hat{\phi}_{2,2} & -\hat{\phi}_{2,1} & 1 & \cdots & 0 \\ \vdots & \vdots & \cdots & \ddots & \vdots \\ -\hat{\phi}_{p-1,p-1} & -\hat{\phi}_{p-1,p-2} & -\hat{\phi}_{p-1,p-3} & \cdots & 1 \end{bmatrix} \tag{12}$$

Stationary stochastic processes: ARMA(p, q) processes

- **ARMA(p, q) process**: The ARMA(p, q) process is generated by the following equation:

$$\phi(L)y_t = \psi(L)\varepsilon_t \tag{13}$$

where $\phi(L) = 1 - \sum_{j=1}^{p} \phi_j L^j$, $\psi(L) = \sum_{j=0}^{q} \psi_j L^j$.

- The process is stationary and invertible if the roots of the $\phi(z)$ and $\psi(z)$ polynomials lie outside the unit circle with MA(∞) $y_t = \phi(L)^{-1}\psi(L)\varepsilon_t = \varphi(L)\varepsilon_t$, where the coefficients φ_j follow from the convolution:

$$(\varphi_0+\varphi_1 z+\varphi_2 z^2 \cdots)\cdot(\phi_0+\phi_1 z+\cdots+\phi_p z^p) = (\psi_0+\psi_1 z+\cdots+\psi_q z^q)$$

such that $\gamma(k) = \sigma^2 \sum_{j=0}^{\infty} \varphi_j \varphi_{j+k}$ and $f(\omega) = \frac{\sigma^2}{2\pi}|\frac{\psi(e^{-\imath\omega})}{\phi(e^{-\imath\omega})}|^2$ (see Def. 3.1.2 and Ths. 3.1.1 and 3.1.2, [BD91]).

Stationary stochastic processes: AR(1) process

- **AR(1) process (red noise)**:

$$y_t = \phi y_{t-1} + \varepsilon_t \qquad \varepsilon_t \sim WN(0, \sigma^2) \tag{14}$$

- The process is stationary if $|\phi| < 1$ with MA(∞) $y_t = \sum_{j=0}^{\infty} \phi^j \varepsilon_{t-j}$. The ACF follows from

$$\begin{array}{rcl} y_t^2 & = & \phi y_{t-1} y_t + \varepsilon_t y_t \quad \Rightarrow E(\cdot) \Rightarrow \quad \gamma(0) \quad = \quad \phi\gamma(1) + \sigma^2 \\ y_t y_{t-1} & = & \phi y_{t-1}^2 + \varepsilon_t y_{t-1} \quad \Rightarrow E(\cdot) \Rightarrow \quad \gamma(1) \quad = \quad \phi\gamma(0) \\ y_t y_{t-k} & = & \phi y_{t-k}^2 + \varepsilon_t y_{t-k} \quad \Rightarrow E(\cdot) \Rightarrow \quad \gamma(k) \quad = \quad \phi^k\gamma(0) \end{array}$$

such that $\gamma(k) = \frac{\sigma^2 \phi^k}{1-\phi^2}$ and
$f(\omega) = \frac{\sigma^2}{2\pi} |(1 - \phi e^{-\imath\omega})|^{-2} = \frac{\sigma^2}{2\pi}(1 - 2\phi\cos(\omega) + \phi^2)^{-1}$

Stationary stochastic processes: AR(1) simulation

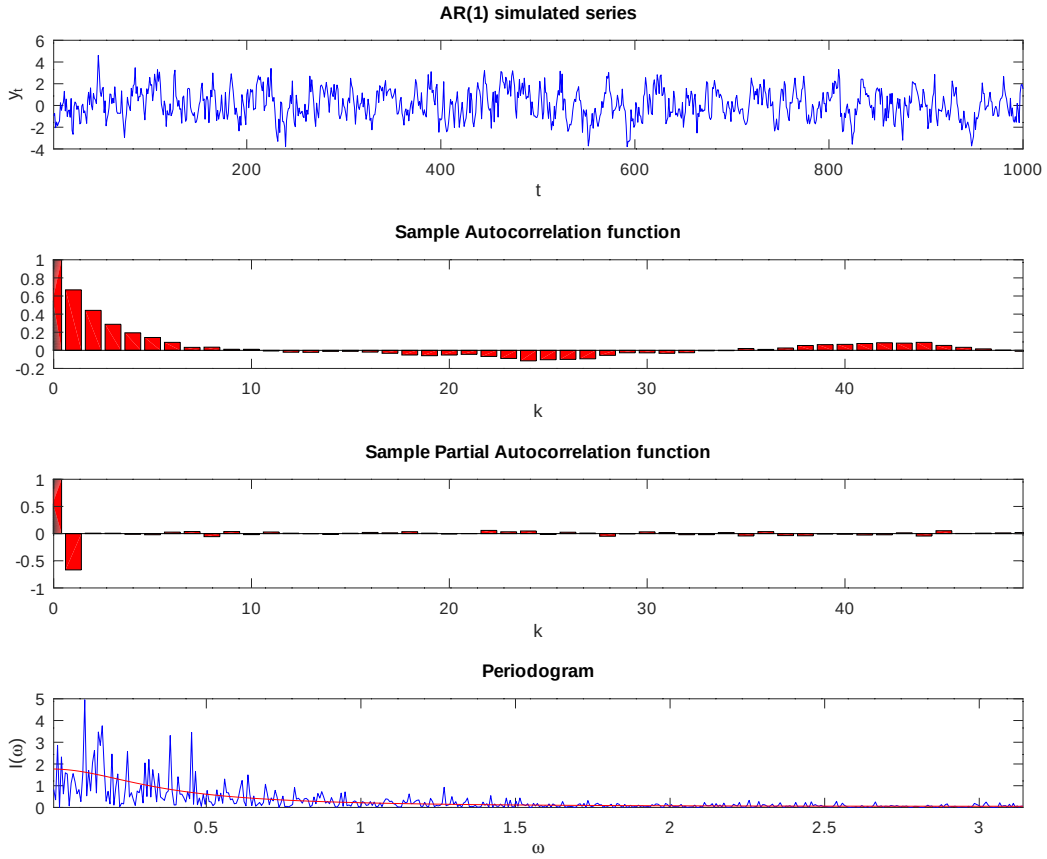

Figure: AR(1) simulation with $\phi = 0.7$ and $\sigma^2 = 1$: time series plot, autocorrelation and periodogram. The red solid line is the theoretical spectral density.

Stationary stochastic processes: Exercise

- Consider the MA(2) process $y_t = \varepsilon_t + \psi_1 \varepsilon_{t-1} + \psi_2 \varepsilon_{t-2}$ with $\varepsilon_t \sim WN(0, \sigma^2)$. Compute the ACF and show that $\gamma(k) = 0$ for $k > 2$. Show that $f(\omega) = \frac{\sigma^2}{2\pi}[1 + \psi_1^2 + \psi_2^2 + 2(\psi_1 + \psi_1\psi_2)\cos(\omega) + 2\psi_2 \cos(2\omega)]$. **Hints**: $e^{-\imath\omega} = \cos(\omega) - \imath \sin(\omega)$, $|a + \imath b| = \sqrt{a^2 + b^2}$ with $a, b \in \mathbb{R}$ and trigonometric identities.
- Simulate the process in OCTAVE considering $\sigma^2 = 1$, $\psi_1 = 0.5$, $\psi_2 = -1.2$ and $n = 1000$. Plot the series, the sample autocorrelation, the sample partial correlation and in the same graph plot the periodogram along to the theoretical spectral density. Why we should deduce from the correlogram that the we have a MA(2) process?

Stationary stochastic processes: Estimation of AR(p)

- **Ordinary least square (OLS):** Regress $\mathbf{y}_{p+1,n} = [y_{p+1}, y_{p+2}, \cdots, y_n]'$ on its past values $\mathbf{X} = [\mathbf{y}_{p,n-1}, \mathbf{y}_{p-1,n-2}, \cdots, \mathbf{y}_{1,n-p}]$:

$$\hat{\phi}_{OLS} = (\mathbf{X}'\mathbf{X})^{-1}\mathbf{X}'\mathbf{y}_{p+1,n} \qquad \hat{\sigma}^2 = \hat{\epsilon}'\hat{\epsilon}/(n-p) \tag{15}$$

  where $\hat{\phi} = [\hat{\phi}_1, \cdots, \hat{\phi}_p]'$ and $\hat{\epsilon} = \mathbf{y}_t - \mathbf{X}\hat{\phi}$.
- **Conditional Sum of Squares (CSS):** Given that $\varepsilon_t \sim N(0, \sigma^2)$, the CSS estimator is $\hat{\phi}_{MLE} = \text{argmax}_{\phi} CSS(\phi)$, where

$$CSS(\phi) = -\frac{n}{2}\log(\sigma^2) - \frac{1}{2\sigma^2}\sum_{j=p+1}^{n}(y_t - \sum_{j=1}^{p}\phi_j y_{t-j})^2 \tag{16}$$

  (see Chapter 8.3,[Has19]).

Stationary stochastic processes: Estimation of AR(p)

- **Maximum Exact Likelihood estimator (MLE):**
  $\mathbf{y} = \begin{bmatrix} y_1, & \cdots & , y_n \end{bmatrix}'$ be n realizations of a random variable $Y \sim N(0, \mathbf{\Gamma}_n(\phi))$. The MLE is $\hat{\phi}_{MLE} = \text{argmax}_{\phi} LL(\phi)$,

$$LL(\phi) = -\frac{n}{2}\log(2\pi) - \frac{1}{2}\mathbf{y}'\mathbf{\Gamma}_n^{-1}(\phi)\mathbf{y} - \frac{1}{2}\log|\mathbf{\Gamma}_n(\phi)| \quad (17)$$

  where the inversion and the determinant of $\mathbf{\Gamma}_n(\phi)$ are computed via the DL algorithm (see Chapter 5, [Ber94]).

Stationary stochastic processes: Estimation of AR(p)

- **Maximum Whittle likelihood estimator (MWLE):** The standard Whittle likelihood is an approximation of the exact log-likelihood where the covariance terms in the time domain are substituted by spectral terms in the frequency domain:

$$L_w(\phi) = -\frac{n}{4\pi}\int_{-\pi}^{\pi} \log f(\omega;\phi)d\omega - \frac{n}{4\pi}\int_{-\pi}^{\pi} \frac{I(\omega)}{f(\omega;\phi)}d\omega \quad (18)$$

  where $f(\omega;\phi)$ is the spectral density and $I(\omega)$ is the periodogram. The main advantage of the Whittle approach is that computations may be simplified considerably with respect to the exact likelihood estimation. The MWLE is $\hat{\phi}_{MWLE} = \text{argmax}_{\phi} L_w(\phi)$ (see Chapter 6, [Ber94])

Stationary stochastic processes: Forecasting the AR(p)

- **Conditional expectation h steps ahead**: Let $\mathcal{I}_t = \{y_t, y_{t-1}, y_{t-2}, \cdots, y_1\}$ be the information set available at time t. The h-steps ahead forecasts follow as

$$
\begin{aligned}
E(y_{t+1}|\mathcal{I}_t) &= \textstyle\sum_{j=1}^{p} \hat{\phi}_j y_{t-j} \\
E(y_{t+2}|\mathcal{I}_t) &= \hat{\phi}_1 E(y_{t+1}|\mathcal{I}_t) + \textstyle\sum_{j=2}^{p} \hat{\phi}_j y_{t-j} \\
E(y_{t+3}|\mathcal{I}_t) &= \textstyle\sum_{j=1}^{2} \hat{\phi}_j E(y_{t+3-j}|\mathcal{I}_t) + \textstyle\sum_{j=3}^{p} \hat{\phi}_j y_{t-j} \\
&\vdots \\
E(y_{t+h}|\mathcal{I}_t) &= \textstyle\sum_{j=1}^{h-1} \hat{\phi}_j E(y_{t+h-j}|\mathcal{I}_t) + \textstyle\sum_{j=h}^{p} \hat{\phi}_j y_{t-j}
\end{aligned}
$$

Stationary stochastic processes: Forecasting the AR(p)

- **The Wiener-Kolmogorov filter**: Let $\mathbf{y}_{n+h} = [y_1, y_2, \cdots, y_n, \cdots, y_{n+h}]'$, then

$$\hat{\mathbf{y}}_{n+h} = \hat{\mathbf{\Gamma}}_{n,n+h} \hat{\mathbf{C}}_n' \hat{\mathbf{D}}_n \hat{\mathbf{C}}_n \mathbf{y}_n \tag{19}$$

  where $\hat{\mathbf{C}}_n' \hat{\mathbf{D}}_n \hat{\mathbf{C}}_n$ is obtained via the DL algorithm using the parametric estimates of the theoretical ACF and $\hat{\mathbf{\Gamma}}_{n,n+h}$ is the $n \times (n+h)$ covariance matrix between $\mathbf{y}_{n+h}$ and $\mathbf{y}_n$ with ij-elements equal to $\hat{\gamma}(|i-j|)$. (see [Pol05]).

Nonstationary processes

- **Integrated process**: An ARMA process is integrated of order $d \in \{1, 2\}$, $y_t \sim I(d)$ or $y_t \sim ARIMA(p, d, q)$, if

$$\phi(L)(1 - L)^d y_t = \psi(L)\varepsilon_t \tag{20}$$

  where if $d = 0$, y_t is the stationary ARMA(p, q) process.

- **Random walk (RW), (Brown noise)**: It is the simplest case with $d = 1$ and $\phi(L) = \psi(L) = 1$:

$$(1 - L)y_t = \varepsilon_t \tag{21}$$

  such that $y_t = y_{t-1} + \varepsilon_t$ and by considering iterative substitutions $y_t = y_0 + \sum_{j=0}^{t-1} \varepsilon_{t-j}$. Such that, assuming y_0 as a known constant

$$\text{Var}(y_t) = t\sigma^2$$

Nonstationary processes

- **Simulating a RW**: Let implement a type I/ type II approach to simulate a RW.
  1. Simulate $5000 + n$ realizations of a gaussian WN, $\varepsilon_t \sim WN(0, \sigma^2)$.
  2. Obtain the type I process $y_t^{(I)} = \sum_{j=0}^{5000+n} \varepsilon_{t-j}$ with $y_0^{(I)} = 0$.
  3. Obtain the type II process by discarding the first 5000 realization.
  4. As a result we obtain n realizations of the RW process

$$y_t = y_0 + \sum_{j=0}^{t-1} \varepsilon_{t-j}$$

with $y_0 = \sum_{j=0}^{4999} \varepsilon_{5000-j}$

Nonstationary processes: Stochastic trend

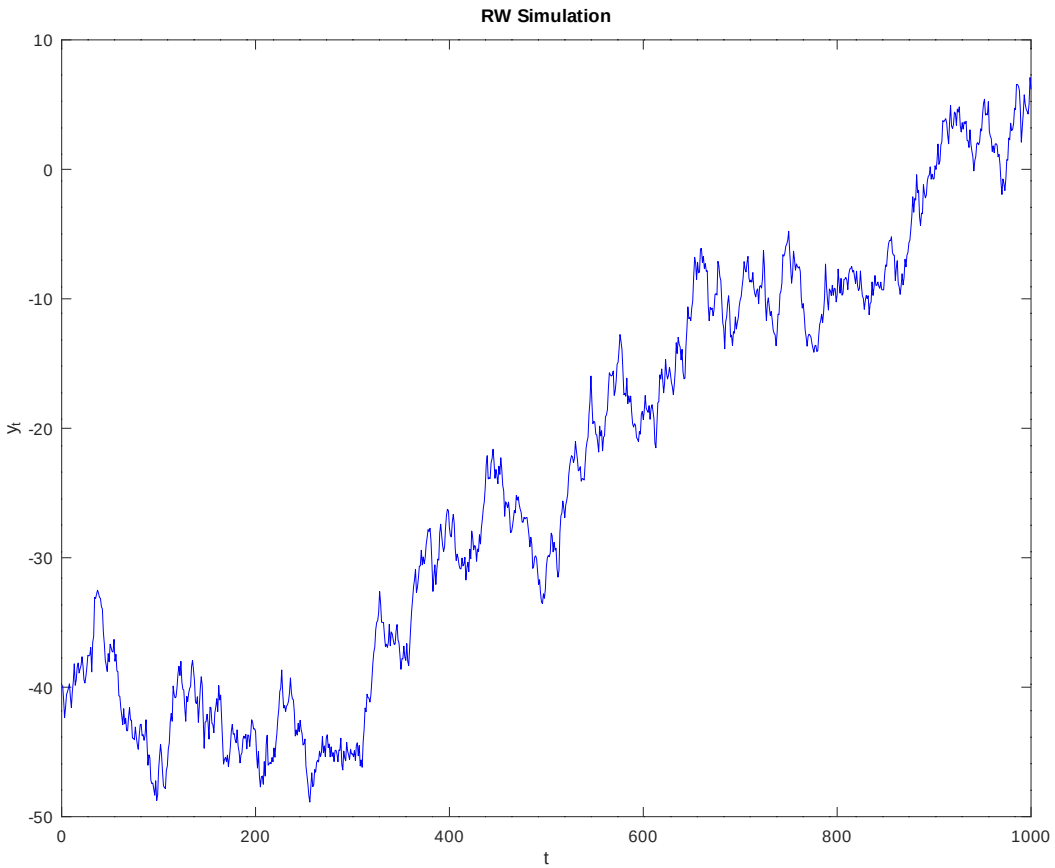

Figure: Simulation of the RW process $y_t = y_{t-1} + \varepsilon_t$. Notice as nonstationarity generates the presence of **stochastic trends**.

Nonstationary processes: First order difference

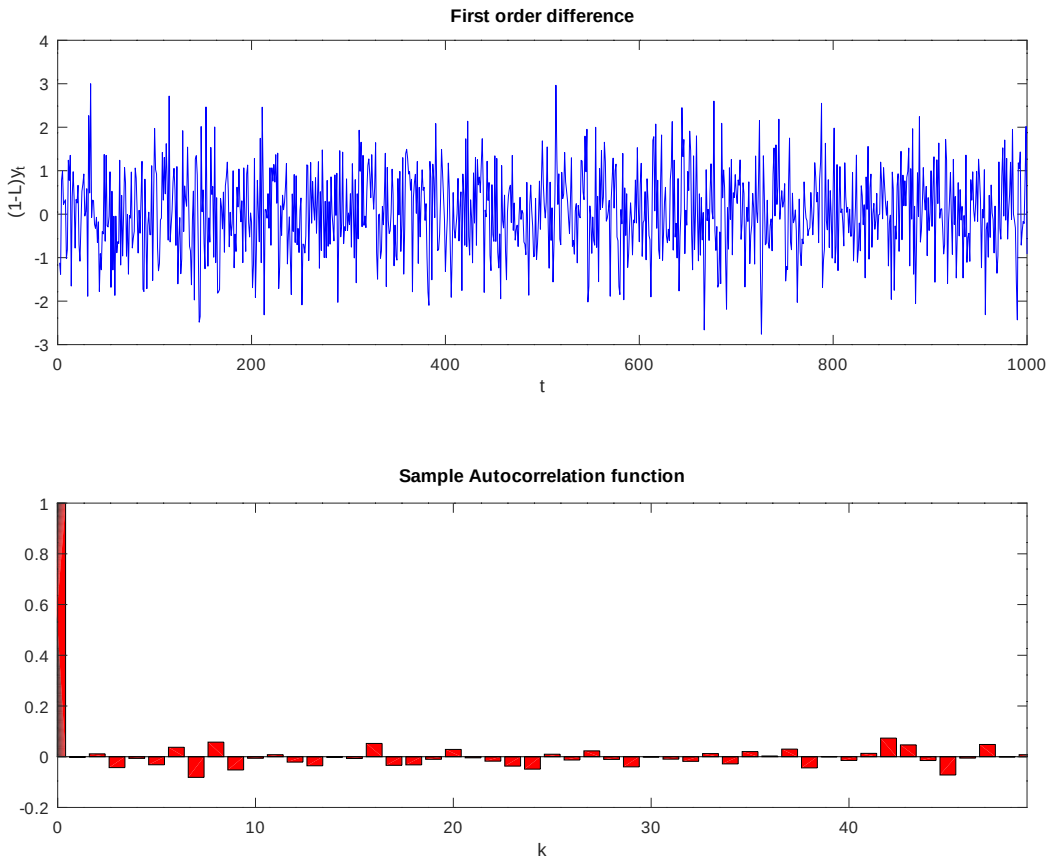

Figure: Notice that applying the first difference to a RW we obtain a WN $e_t = y_t - y_{t-1} = (1-L)y_t$. The filter $(1-L)^d$ is often used to remove nonstationarity.

Deterministic trends

- The simplest model for a deterministic trends is given by the following p-order polynomial

$$\mu_t = \beta_0 + \beta_1 t + \beta_2 t^2 + \cdots + \beta_p t^p \tag{22}$$

- Adding a stochastic component, e.g. a red noise component, we obtain the following signal plus noise model

$$\begin{aligned} y_t &= \mu_t + x_t \\ x_t &= \phi x_{t-1} + \varepsilon_t \end{aligned} \tag{23}$$

which can be estimated via OLS.

Deterministic trends: simulation.

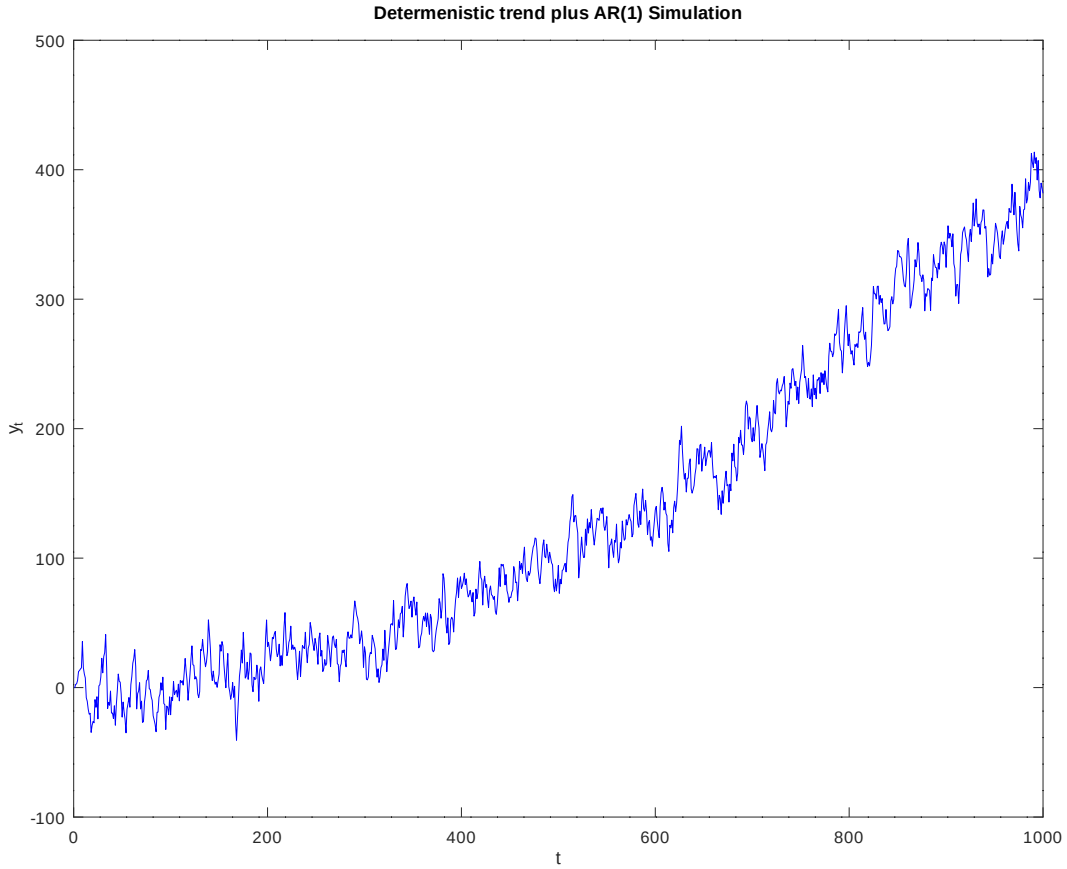

Figure: Simulation of a quadratic trend plus red noise process.

Long Memory processes

- **Long memory** A stationary stochastic process y_t with ACF $\gamma(k)$ and spectral density $f(\omega)$ exhibits long memory if $\sum_{k=0}^{\infty} |\gamma(k)| = \infty$ or, equivalently, $f(\omega_0) = \infty$ for some $\omega_0 \in [0, \pi]$. Otherwise the process displays short memory (see Chapter 2, [Has19]).
- **FARIMA processes**: Let $d \in (-1, 1)$, then $y_t \sim FARIMA(p, d, q)$ with

$$\phi(L)(1 - L)^d y_t = \psi(L)\varepsilon_t \tag{24}$$

such that if $d = 0$, y_t is the stationary ARMA(p, q) process (see [Hos81]).

Long Memory processes

- **Fractional noise (pink noise)**: The simplest case is obtained with $\phi(L) = \psi(L) = 1$ and $d \in (-1, 1)$, then $y_t \sim FN(d)$ such that
$$(1 - L)^d y_t = \varepsilon_t \tag{25}$$
with spectral density $f(\omega) = \frac{\sigma^2}{2\pi}\left(4\sin^2(\frac{\omega}{2})\right)^{-d}$ and ACF
$$\gamma(k) = \sigma^2 \frac{\Gamma(1-2d)\Gamma(d+k)}{\Gamma(k+1-d)\Gamma(d)\Gamma(1-d)}, \tag{26}$$
where $\Gamma(u) = \int_0^\infty z^{u-1}e^{-z}dz$ is the Euler Gamma function (see [And86]).
- The MA(∞) representation is obtained from the binomial expansion $(1-L)^{-d} = \sum_{j=0}^{\infty} \frac{\Gamma(j+d)}{\Gamma(j+1)\Gamma(d)} L^j$. The AR($\infty$) representation follows directly.

Long Memory processes

- The FN is stationary and exhibits long memory if $d \in (0, 1/2)$, in fact $f(\omega) \sim \omega^{-2d}$ as $\omega \to 0$ and $\gamma(k) \sim \frac{k^{2d-1}}{\Gamma(d)}$ as $k \to \infty$, which follows from $\frac{\Gamma(k+d+j)}{\Gamma(k+1-d)} \sim k^{2d-1+j}$ and $\frac{\Gamma(k+1-d+j)}{\Gamma(k+1-d)} \sim k^j$.
- Otherwise, the FN process is nonstationary under long memory if $d > 1/2$ (see [VR00]).
- **Comparison with the AR(1):** If $y_t \sim AR(1)$ then $f(0) = \frac{\sigma^2}{2\pi}(1-\phi^2)^{-2}$ and $\sum_{k=0}^{\infty} |\gamma(k)| = \frac{\sigma^2}{1-\phi^2} \sum_{k=0}^{\infty} |\phi^k| < \infty$, such that the AR(1) process is short memory.

Long Memory processes: FN simulation

- **Simulation via the DL method:** Let $\mathbf{y} = \begin{bmatrix} y_1, & \cdots & , y_n \end{bmatrix}'$ be n realizations of the FN process $\mathbf{y} \sim N(0, \mathbf{\Gamma}_n)$ where $\mathbf{\Gamma}_n^{-1} = \mathbf{C}_n' \mathbf{D}_n \mathbf{C}_n$ and let $\boldsymbol{\varepsilon} = \begin{bmatrix} \varepsilon_1, & \cdots & , \varepsilon_n \end{bmatrix}'$ distributed as $\boldsymbol{\varepsilon} \sim N(0, I_n)$. Notice that $\mathbf{C}_n \mathbf{y} = \mathbf{D}_n^{-\frac{1}{2}} \boldsymbol{\varepsilon}$ leads to the system of equations

$$\begin{aligned} y_1 &= \sqrt{v_0}\varepsilon_1 \\ y_2 &= \phi_{1,1} y_1 + \sqrt{v_1}\varepsilon_2 \\ y_3 &= \phi_{2,1} y_2 + \phi_{2,2} y_1 + \sqrt{v_2}\varepsilon_3 \\ &\vdots \\ y_t &= \phi_{t-1,1} y_{t-1} + \cdots + \phi_{t-1,t-1} y_1 + \sqrt{v_{t-1}}\varepsilon_t \end{aligned} \tag{27}$$

for $t = 1, \cdots, n$, such that the FN process can be simulated via

$$\mathbf{y} = \mathbf{C}_n^{-1} \mathbf{D}_n^{-\frac{1}{2}} \boldsymbol{\varepsilon}$$

Long Memory processes: FN simulation

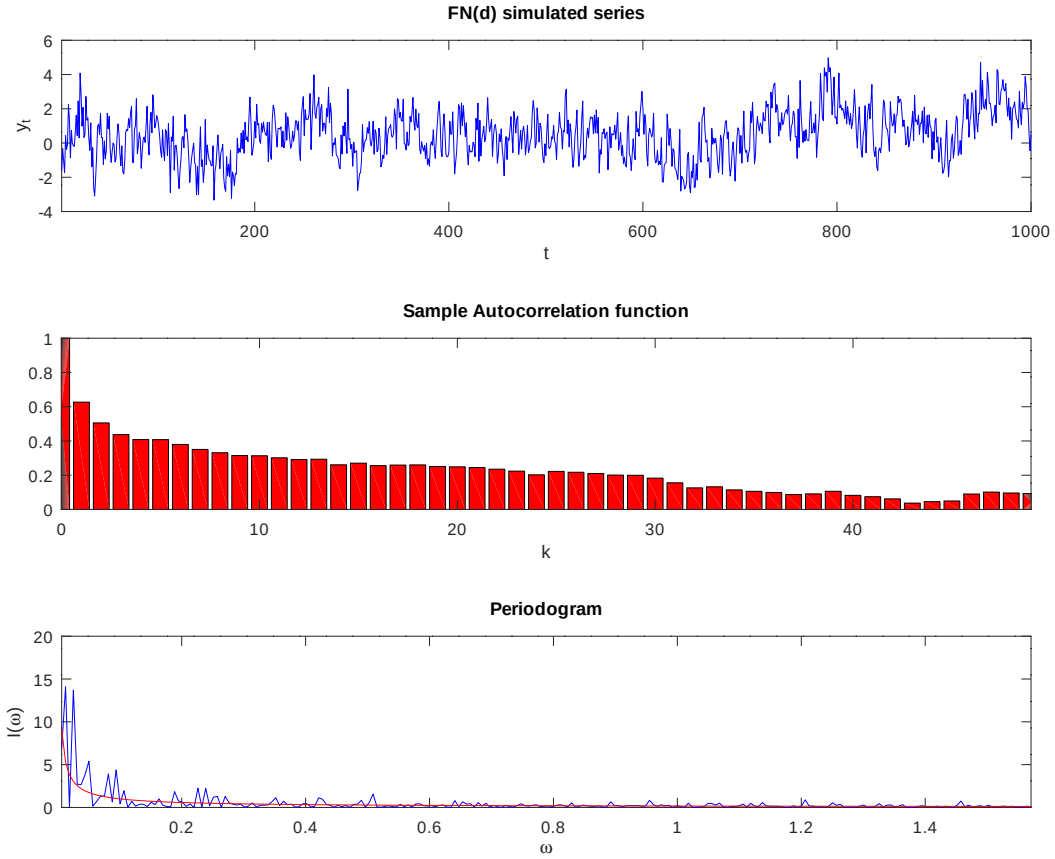

Figure: FN simulation with $d = 0.4$ and $\sigma^2 = 1$: time series plot, autocorrelation and periodogram. The red solid line is the theoretical spectral density.

Long Memory processes: Exercise

Implement a Monte Carlo experiment with 1000 reps. For each reps:

1. First simulate $n = 400$ realizations from the random process with occasional shifts in the mean:

$$y_t = \varepsilon_t + \sum_{i=1}^{t} \eta_i b_i \tag{28}$$

   where $\varepsilon_t \sim N(0,1)$, $\eta_t \sim N(0, 0.1)$, $E(\varepsilon_t \eta_t) = 0$ and b_i follows an i.i.d. binomial distribution with $p = \text{Prob}(b_i = 1)$ representing the probability of a break and η_t establishes the size of its jump, such that pn returns the expected number of breaks. (**Hints**: use the function binornd()).

2. Then estimate at each reps the FN model.

Finally, compute the Monte Carlo mean $E(\hat{d})$ of the memory parameters on all the 1000 reps. Repeat the experiment for the values of $p \in \{0.05, 0.15, 0.25\}$.

What are the conclusions of the experiments as pn increases?

Long Memory processes: Empirical application on tree rings records

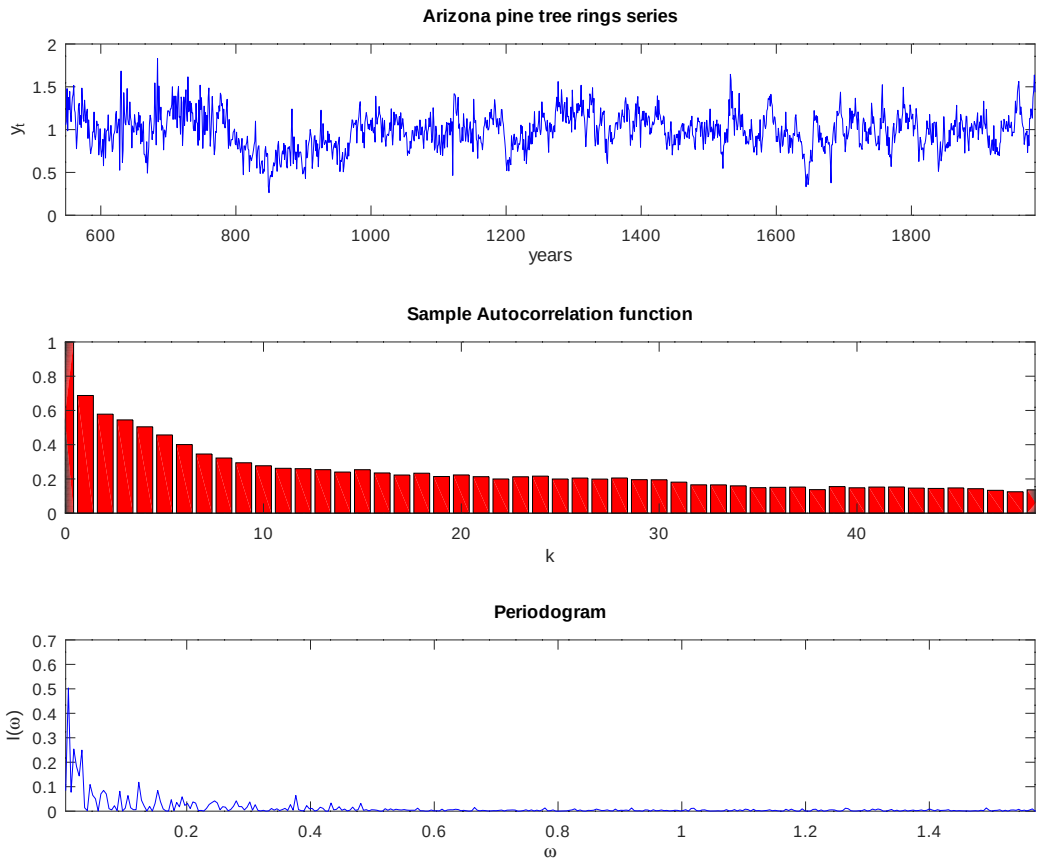

Figure: Arizona pine tree rings yearly records: time series plot, correlogram and periodogram.

Long Memory processes: Empirical application on tree rings records

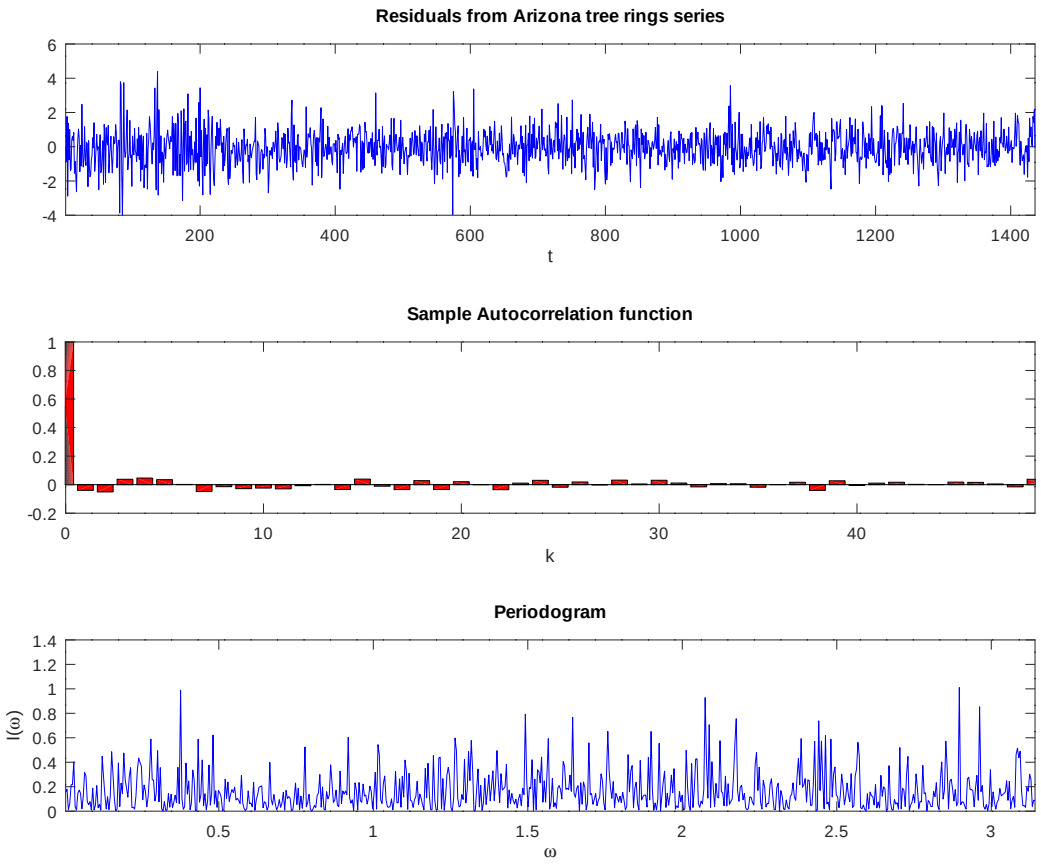

Figure: Residuals $\hat{\varepsilon} = \hat{\mathbf{D}}^{\frac{1}{2}}\hat{\mathbf{C}}^{-1}\mathbf{y}$ obtained via the Whittle estimation of the FN model on the Arizona pine tree rings series. The estimate parameters are $\hat{d} = 0.54$ and $\hat{\sigma}^2 = 0.02$.

Long Memory processes: Empirical application on tree rings records

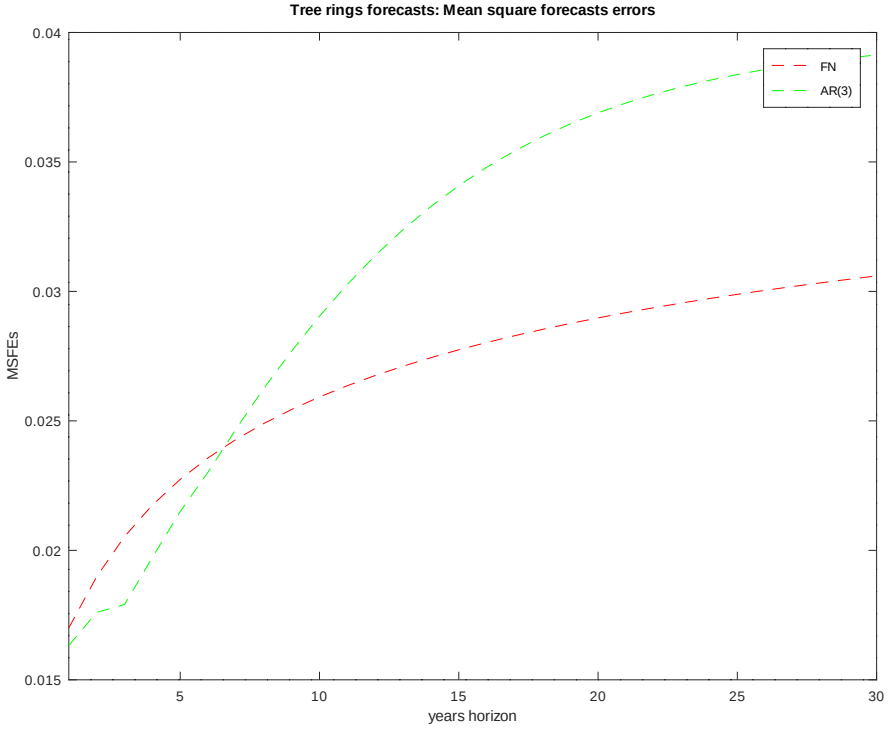

Figure: Comparison between the mean square forecast errors (MSFEs) obtained by forecasting h-steps ahead (for $h = 1, 2, \cdots, 30$) the yearly tree rings series via the FN and AR(3) models. Forecasts are based on the initial estimation of the two models on the first 1336 observation. Then predictions yielded on the remaining 100 years.

Cyclical processes: Deterministic cycles

- **The harmonic model:** The most used model for deterministic cycles in environmental time series is the harmonic process

$$y_t = \cos(\lambda t)\alpha + \sin(\lambda t)\alpha^* \tag{29}$$

which reduces to the sinusoidal wave

$$y_t = A\cos(\lambda t + \varpi) \tag{30}$$

where $\varpi = \arctan(-\alpha^*/\alpha)$ is the phase and $A = \sqrt{\alpha^2 + \alpha^{2*}}$ is the amplitude of the wave.

- Let $\alpha, \alpha^* \sim N(0, \sigma_\alpha^2)$. Then $E(y_t y_{t-k}) = \gamma(k) = \sigma_\alpha^2 \cos(\lambda k)$.
- The model allows for multiple periodicities at $P_j = 2\pi/\lambda_j$ with $\lambda_j \in (0, \pi)$ for $j = 1, \cdots, k$ via aggregation by sum according to

$$y_t = \sum_{j=1}^{k} \cos(\lambda_j t)\alpha_j + \sin(\lambda_j t)\alpha_j^* \tag{31}$$

such that the α_j and α_j^* can be estimated by regressing y_t on the Fourier terms.

Cyclical processes: Deterministic cycles

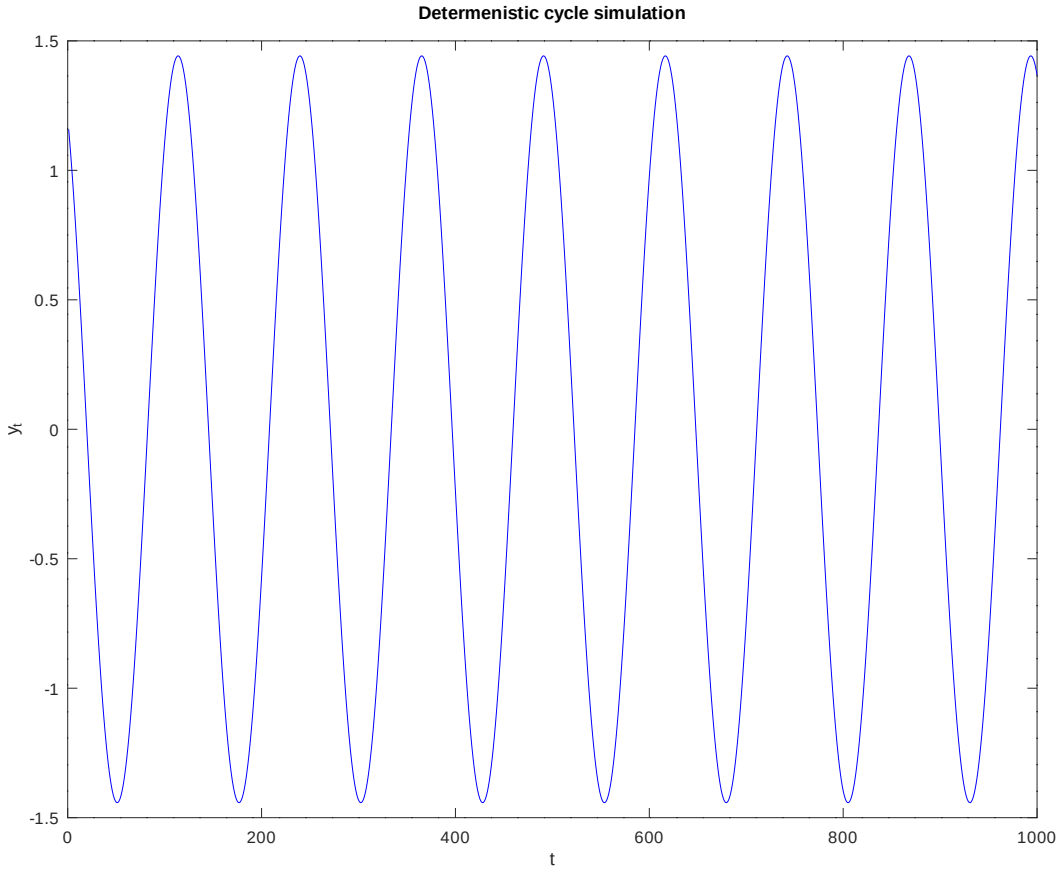

Figure: Simulation of the harmonic process with $\alpha = 1.3$, $\alpha^* = -0.8$ and $\lambda = 0.05$.

Cyclical processes: the SARIMA model

- **SARIMA model:** A general SARIMA model can be represented by

$$(1-L)(1-L^s)(1-\phi_s L^s)y_t = (1-\psi_s L^s)\frac{\psi(L)}{\phi(L)}\varepsilon_t \qquad (32)$$

  which exhibits seasonality with period $s \in \mathbb{N}$ such that the spectral density displays peaks at the frequencies $2\pi j/s$ for $j = 1, 2, \cdots, [s/2]$ (e.g. if y_t is monthly recorded then $s = 12$ means a yearly seasonality).

- **Particular case:** Consider the special case

$$(1-\phi_s L^s)y_t = \varepsilon_t, \qquad (33)$$

  with spectral density $f(\omega) = \frac{\sigma^2}{2\pi}(1 - 2\phi_s \cos(s\omega) + \phi_s^2)^{-1}$ and ACF $\gamma(sk) = \sigma^2 \frac{\phi_s^k}{1-\phi_s^2}$ for $sk = 0, s, 2s, \cdots$ and 0 otherwise. Estimation can be easily carried out via the CSS method.

Cyclical processes: SARIMA simulation

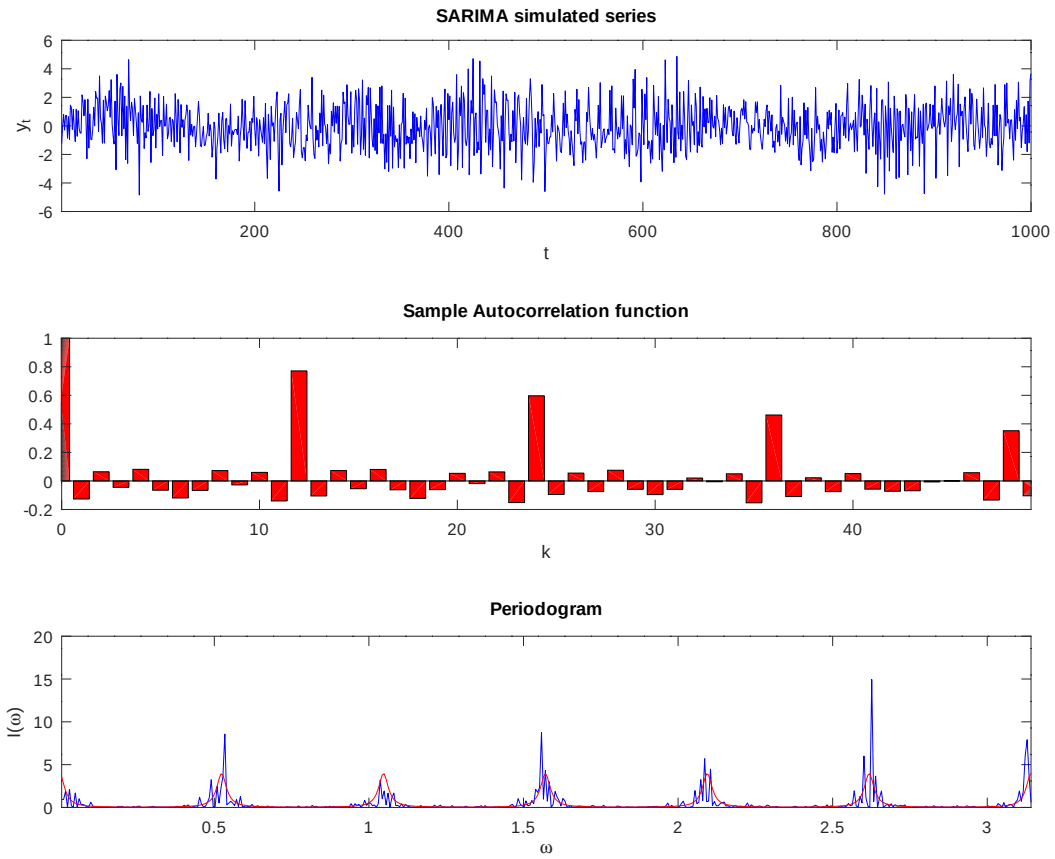

Figure: Simulation of the seasonal model $(1 - \phi_s L^s) y_t = \varepsilon_t$, with $s = 12$, $\phi_s = 0.8$ and $\sigma^2 = 1$: time series plot, autocorrelation and periodogram. The red solid line is the theoretical spectral density.

Cyclical processes: short memory cycles

- The following AR(2) process is a model for stationary short memory stochastic cycle:

$$y_t = 2\rho\cos(\lambda)y_{t-1} - \rho^2 y_{t-2} + \varepsilon_t \tag{34}$$

  with $|\rho| < 1$, the spectral density is continuous and bounded, with a peak around the frequency λ.
- Notice that the AR polynomial has complex conjugate roots $z_{1,2} = \frac{\cos(\lambda)\pm\sqrt{\cos^2(\lambda)-1}}{\rho}$ for $\lambda \in (0, \pi)$. Each AR(2) with complex conjugate roots exhibits periodicity (see [GHR01]).
- The process is nonstationary for $\rho = 1$.

Cyclical processes: long memory cycles

- A process for long memory cycles is represented by the **Gegenbauer process** (c.f. [GZW89]):

$$(1 - 2\cos(\lambda)L + L^2)^d y_t = \varepsilon_t \tag{35}$$

  which is stationary under long memory if $\lambda \in (0, \pi)$ and $d \in (0, 1/2)$ or $\lambda \in \{0, \pi\}$ and $d \in (0, 1/4)$.
- The spectral density is unbounded at the λ frequency:

$$f(\omega) = \frac{\sigma^2}{2\pi} |2\sin(\frac{\omega - \lambda}{2})|^{-2d} |2\sin(\frac{\omega + \lambda}{2})|^{-2d} \tag{36}$$

- The process can be generalized for multiple periodicities at $P_j = 2\pi/\lambda_j$ for $j = 1, \cdots, k$ via the k-factor Gegenbauer model:

$$\prod_{j=1}^{k} (1 - 2\cos(\lambda_j)L + L^2)^{d_j} y_t = \varepsilon_t \tag{37}$$

- One limitation of the Gegenbauer process is the lack of a closed form expression for the ACF. This prevents exact maximum likelihood estimation and optimal signal extraction.

Cyclical processes: long memory cycles

- **The fractional sinusoidal waveform (fSW) process**: Consider the harmonic process $y_t = \alpha \cos(\lambda) + \alpha^* \sin(\lambda)$ with $\lambda \in [0, \pi]$, the fSW process is defined by the modulation of the trigonometric functions by two independent fractional noise processes, such that:

$$\begin{aligned} y_t &= \alpha_t \cos(\lambda t) + \alpha_t^* \sin(\lambda t) \\ (1-L)^d \alpha_t &= \eta_t \\ (1-L)^d \alpha_t^* &= \eta_t^* \end{aligned} \tag{38}$$

where $\eta_t, \eta_t^* \sim N(0, \sigma_\eta^2)$ (see [PM22]). The fSW process displays long memory under stationarity if $d \in (0, 1/2)$. The ACF and spectral density are

$$\gamma(k) = \sigma_\eta^2 \frac{\Gamma(1-2d)\Gamma(d+k)}{\Gamma(k+1-d)\Gamma(d)\Gamma(1-d)} \cos(\lambda k) \tag{39}$$

$$f(\omega) = \frac{\sigma^2}{4\pi} \left[(2\sin(\frac{\omega - \lambda}{2}))^{-2d} + (2\sin(\frac{\omega + \lambda}{2}))^{-2d} \right] \tag{40}$$

Cyclical processes: long memory cycles

- **Deterministic cycles** arise as a limiting case of the fSW process. Consider again the ACF of the fSW process, and define $\sigma_\alpha^2 = \sigma_\eta^2 \frac{\Gamma(1-2d)}{\Gamma^2(1-d)}$. Assume that for a positive constant c we can write $\sigma_\eta^2 = c(1-2d)\pi$. Then, if $d \to \frac{1}{2}$ from the left, $\lim_{d \to \frac{1}{2}-} \sigma_\alpha^2 = c > 0$ (as $\lim_{x \to 0^+} x\Gamma(x) = 1, x = 1-2d$). Moreover, the ACF

$$\gamma(k) = \sigma_\alpha^2 \frac{\Gamma(1-d)\Gamma(d+k)}{\Gamma(1+k-d)\Gamma(d)} \cos(\lambda k), \sigma_\alpha^2 > 0,$$

for $d \to (1/2)^-$, tends to $\gamma(k) = \sigma_\alpha^2 \cos(\lambda k)$. Hence, when $\sigma_\eta^2 \to 0$ and $d \to \frac{1}{2}$ from the left, the fSW process has the same ACF of the harmonic process.

Cyclical processes: long memory cycles

- **Multiple periodicities**: Let $\lambda_j \in [0, \pi]$ for $j = 1, \cdots, k$, the following specification may be suitable for periodic time series with periods $P_j = 2\pi/\lambda_j$:

$$\begin{aligned} y_t &= \mu + \sum_{j=1}^{k} \left(\alpha_{jt} \cos(\lambda_j t) + \alpha^*_{jt} \sin(\lambda_j t) \right), \\ \alpha_{j,t} &= (1-L)^{-d_j} \eta_{j,t} \\ \alpha^*_{j,t} &= (1-L)^{-d_j} \eta^*_{j,t} \end{aligned} \tag{41}$$

  where $\eta_{j,t}, \eta^*_{j,t} \sim i.i.d. N(0, \sigma^2_{\eta j})$.
- In contrast with the Gegenbauer process, the ACF is available in a simple and closed form, allowing for model estimation via exact likelihood and optimal signal extraction, obtained via the support of the DL algorithm.
- The model introduces multiple sources of disturbances at the different frequencies, allowing for more flexibility.
- Defining $\sigma^2_{\alpha j} = \sigma^2_{\eta j} \frac{\Gamma(1-2d_j)}{\Gamma^2(1-d_j)}$ the model allows for an easy decomposition of the variance of the process in the variability of each j components such that $\gamma(0) = \sum_{j=1}^{k} \sigma^2_{\alpha j}$.

Cyclical processes: signal extraction

- Consider the following process with unobserved components:

$$\begin{aligned} y_t &= s_t + x_t \\ s_t &= \alpha_t \cos(\lambda t) + \alpha_t^* \sin(\lambda t) \\ (1-L)^d \alpha_t &= \eta_t \\ (1-L)^d \alpha_t^* &= \eta_t^* \\ (1-\phi L) x_t &= \varepsilon_t \end{aligned} \tag{42}$$

  with $\eta_t, \eta_t^* \sim i.i.d.N(0, \sigma_\eta^2)$ and $\varepsilon_t \sim i.i.d.N(0, \sigma^2)$.

- Signal extraction of the unobserved components can be implemented via the **Wiener-Kolmogorov filter**:

$$\begin{aligned} \hat{\mathbf{s}} &= \hat{\mathbf{\Gamma}}_{s,y} \hat{\mathbf{C}}_n' \hat{\mathbf{D}}_n \hat{\mathbf{C}}_n \mathbf{y} & \hat{\Gamma}_{s,y}(i,j) &= \frac{\hat{\sigma}_\eta^2 \Gamma(1-2\hat{d}) \Gamma(\hat{d}+|i-j|) \cos(\lambda |i-j|)}{\Gamma(|i-j|+1-\hat{d}) \Gamma(\hat{d}) \Gamma(1-\hat{d})} \\ \hat{\mathbf{x}} &= \hat{\mathbf{\Gamma}}_{x,y} \hat{\mathbf{C}}_n' \hat{\mathbf{D}}_n \hat{\mathbf{C}}_n \mathbf{y} & \hat{\Gamma}_{x,y}(i,j) &= \frac{\hat{\sigma}^2 \hat{\phi}^{|i-j|}}{1-\hat{\phi}^2} \end{aligned}$$

Cyclical processes: signal extraction

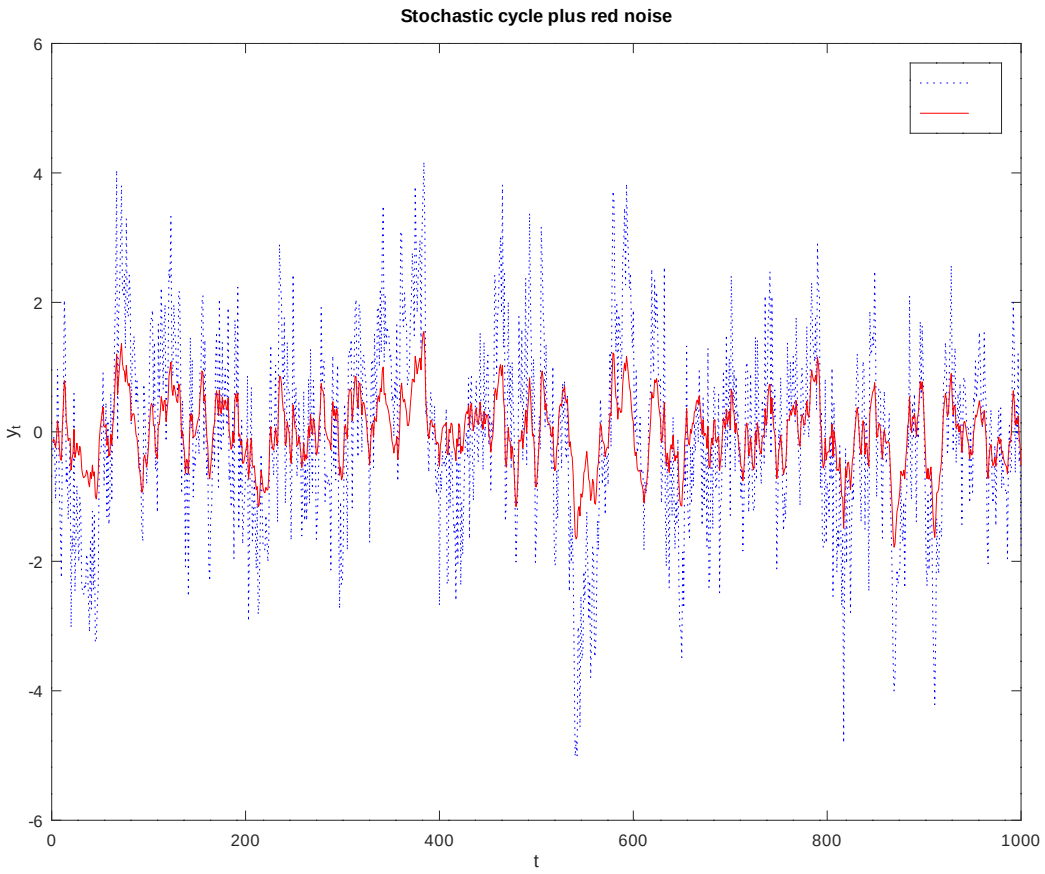

Figure: Simulation of the fSW plus red noise model (dotted blue line) and extraction of the red noise component (solid red line) via the Wiener-Kolmogorov filter once the model's parameters have been estimated via exact maximum likelihood..

Cyclical processes: Empirical application on Mauna Loa

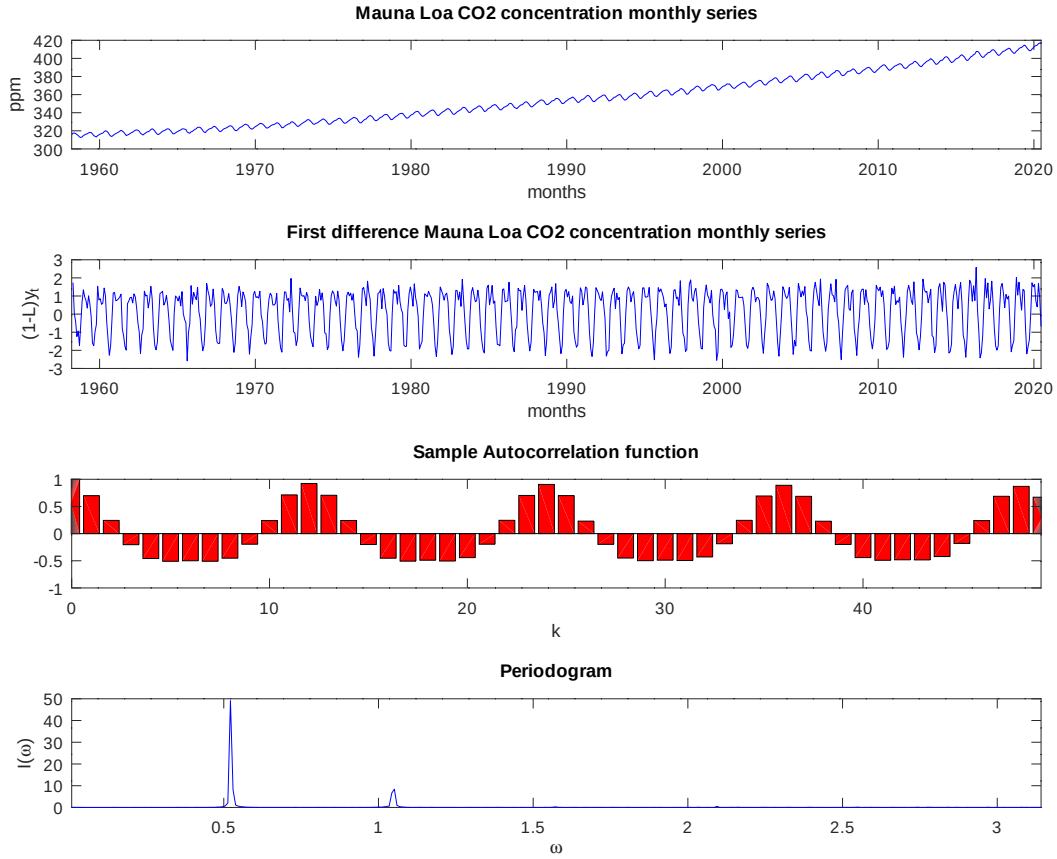

Figure: CO2 concentration ppm recorded at the observatory of Mauna Loa (Hawaii): Time series plot of y_t, first difference of the series $(1-L)y_t$, correlogram and periodogram of $(1-L)y_t$.

Cyclical processes: Empirical application on Mauna Loa

- The series is very relevant for climate change discussion, being the longest instrumental record available of atmospheric CO_2.
- While its distinctive upward pattern is attributed to anthropogenic causes (combustion of fossil fuels and long-term changes in land use), the series displays important inter-annual and intra-annual movements.
- The seasonal cycle, which peaks in May and has a trough in October, is driven by the metabolic activity of terrestrial plants and soils: the process of carbon uptake and release of the land biosphere is such that CO_2 concentrations increase in winter, when plant respiration dominates, and decreases in summer, when the photosyntesis uptake dominates.

Cyclical processes: Empirical application on Mauna Loa

Two models will be fitted for this series:

- SARIMA model estimated via the CSS methodology.

$$(1-\phi L-\Phi L^{12})(1-L)(1-L^{12})y_t=(1-\theta L-\Theta L^{12})\varepsilon_t$$

  with $|\phi|<1, |\Phi|<1$, $|\theta|<1$, $|\Theta|<1$.

- fSW model estimated via exact likelihood

$$y_t=\beta_0+\beta_1 t+\beta_2 t^2+\alpha_{0t}+\sum_{j=1}^{6}\Big(\alpha_{jt}\cos(\lambda_j t)+\alpha^*_{jt}\sin(\lambda_j t)\Big)$$

  where $\lambda_j=2\pi j/12$ for $j=1,\cdots,6$ is the annual frequency and $(1-\phi L)\alpha_{0t}=\varepsilon_t$ is a red noise component.

Cyclical processes: Empirical application on Mauna Loa

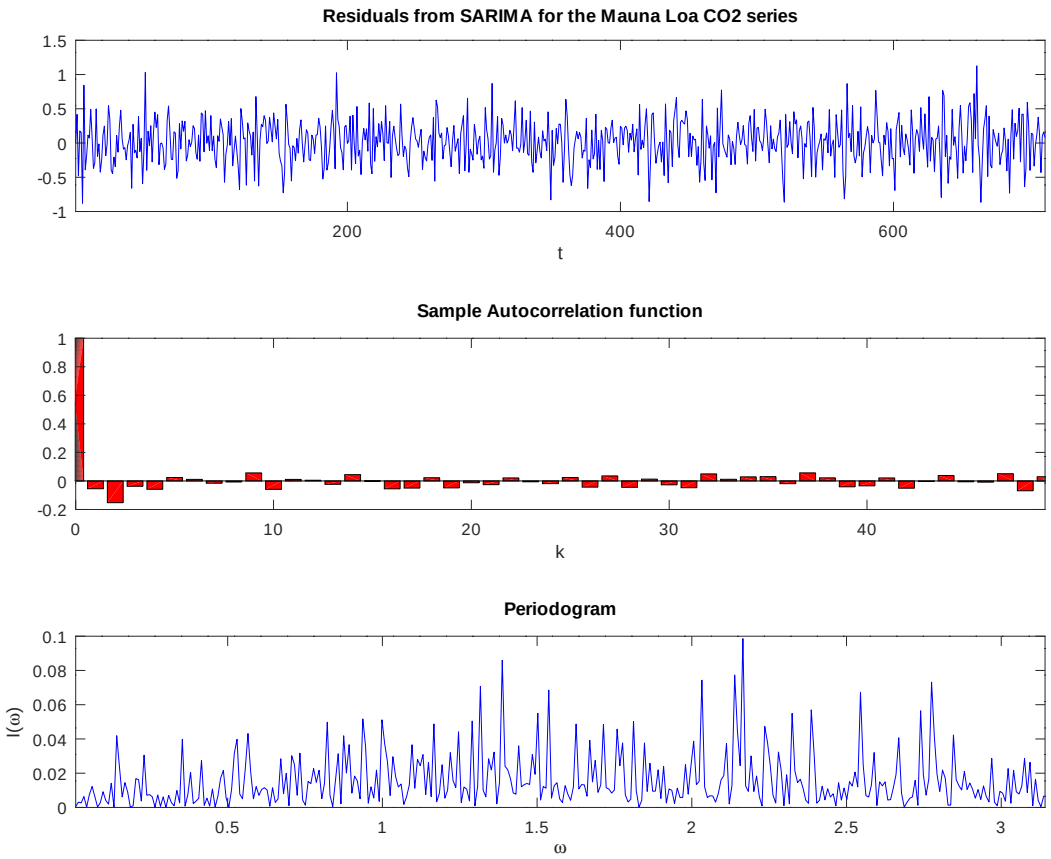

Figure: Residuals obtained from the SARIMA specification: time series plot, correlogram and periodogram. The coefficient of determination $R^2 = 1 - \sum_{t=1}^{n} \hat{\epsilon}_t^2 / \sum_{t=1}^{n} (y_t - \bar{y})^2$ on the detrended series is 0.9368.

Cyclical processes: Empirical application on Mauna Loa

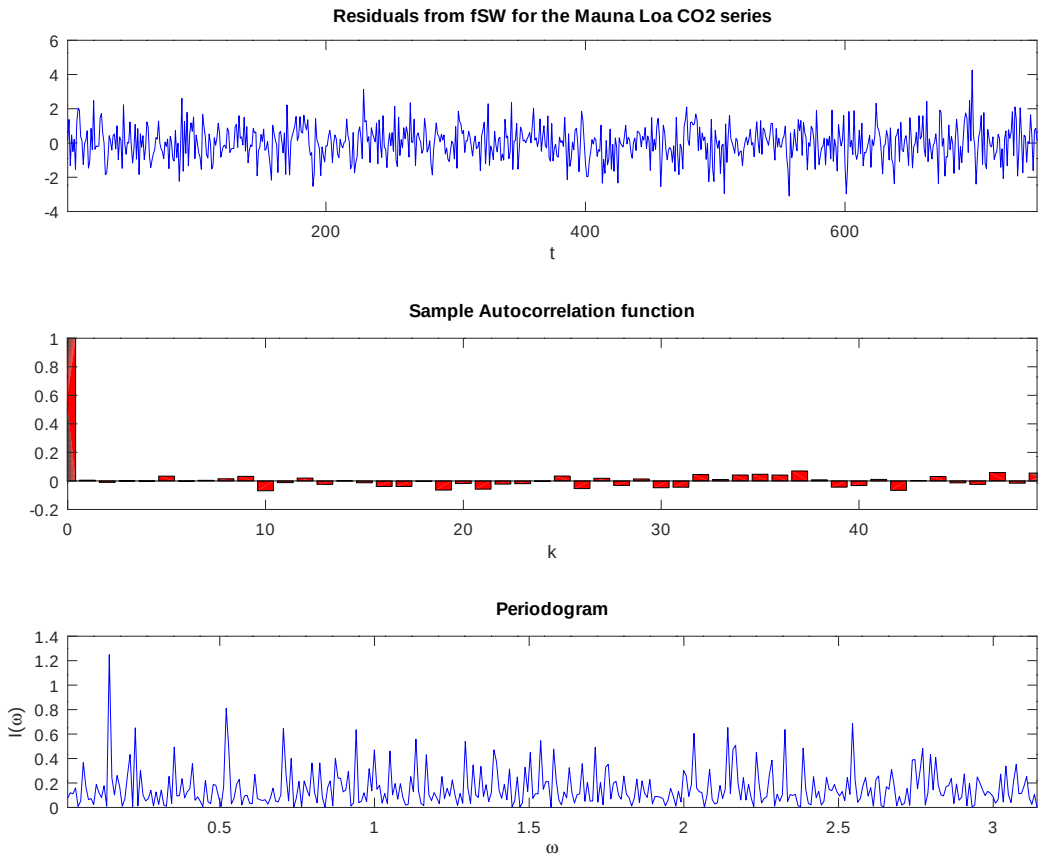

Figure: Residuals obtained from the fSW specification: time series plot, correlogram and periodogram. The coefficient of determination $R^2 = 1 - \sum_{t=1}^{n} \hat{\epsilon}_t^2 / \sum_{t=1}^{n} (y_t - \bar{y})^2$ on the detrended series is 0.9799.

Cyclical processes: Empirical application on Mauna Loa

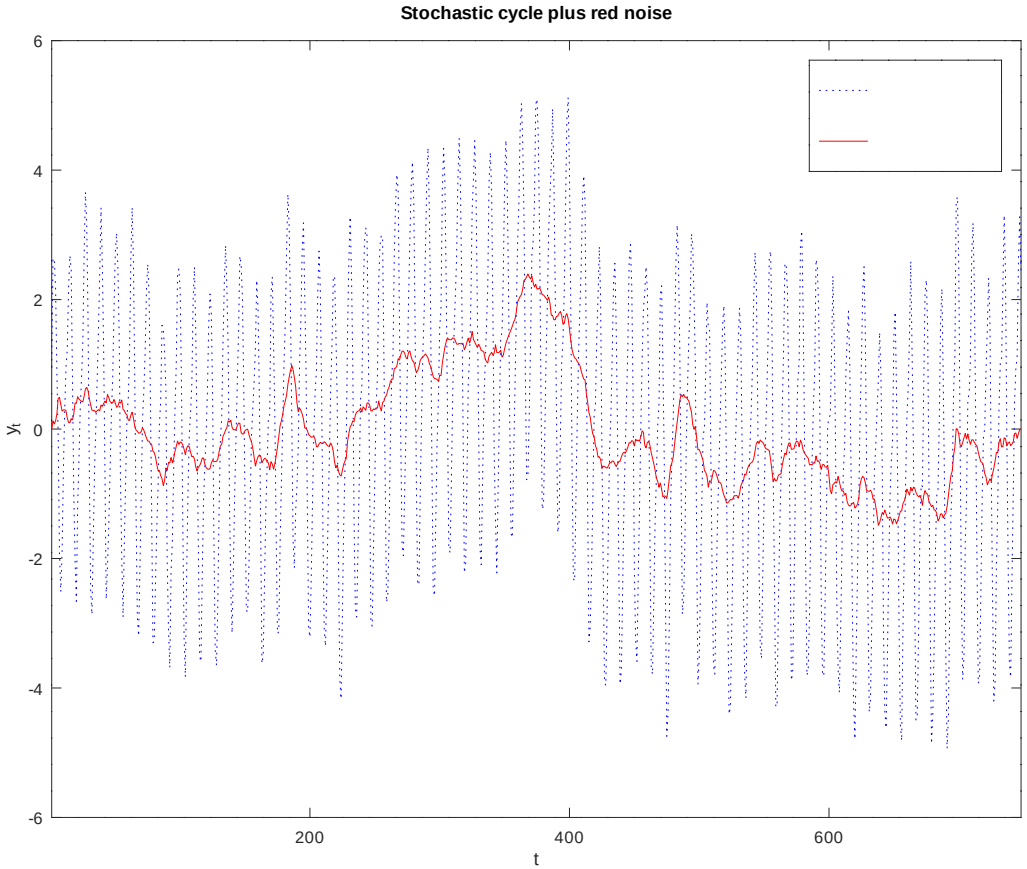

Figure: Extraction of the long run component (red noise, red solid line) via the fSW specification, describing the underlying climate pattern. The blue dotted line in the background is the detrended series.

Cyclical processes: Empirical application on Ice cores

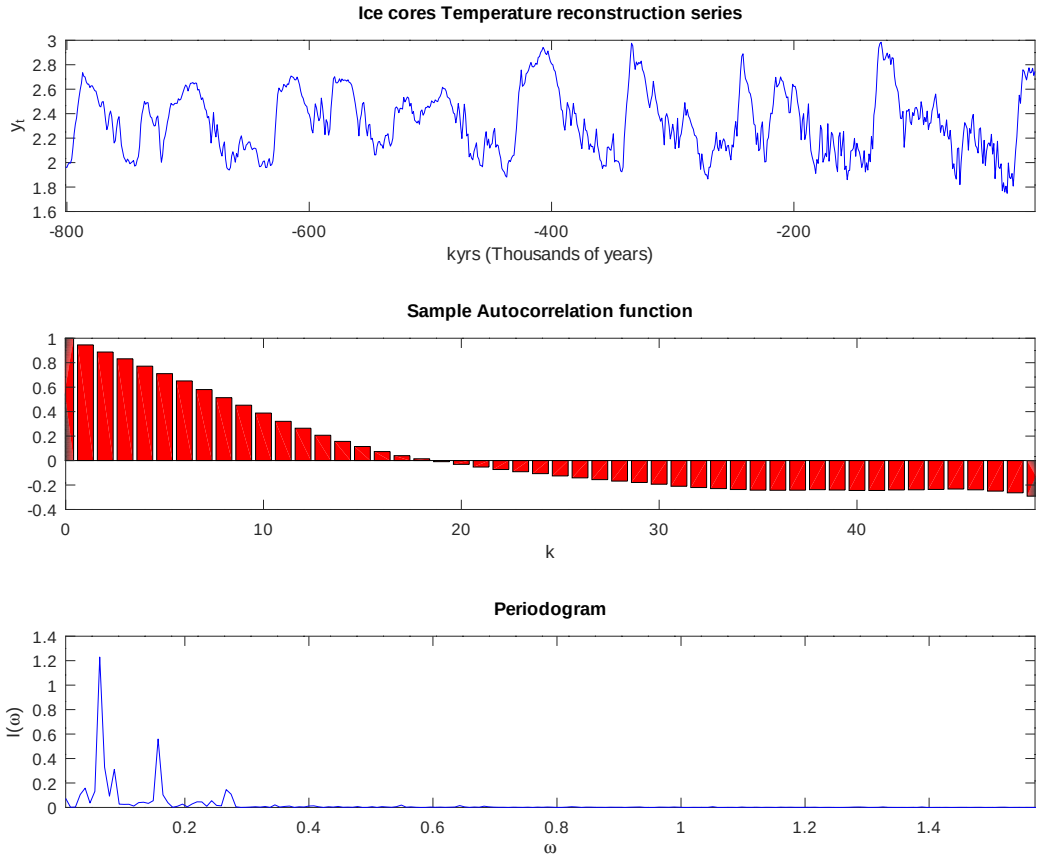

Figure: Temperature reconstruction obtained from the ice cores records collected at the South pole station EPICA Dome C: time series plot, correlogram and periodogram.

Cyclical processes: Empirical application on Ice cores

- The series displays substantial recurrent co-movements referred to as *glacial cycles*: during glaciations, temperature stay below its mean for prolonged periods.
- According to the paleoclimatic literature and the Milankovitch theory, glacial cycles are attributed to changes in Earth's orbital geometry over time, which affects incoming solar radiation.
- The three main sources of variation are: i. eccentricity of the Earth orbit round the Sun, due to gravitational effects of other planets in the solar system, which varies deterministically with a periodicity of about 100 kyr; ii. obliquity or tilt of the Earth's axis of rotation, which varies with a period of 41 kyr; iii. precession of the equinoxes. This component has periodicities of about 23 and 19 kyr.

Cyclical processes: Empirical application on Ice cores

Setting $[\lambda_1, \lambda_2, \lambda_3, \lambda_4] = 2\pi/[100, 41, 23, 19]$, two models will be fitted for this series:

- Harmonic model plus red noise estimated into two step via OLS and exact likelihood estimation.

$$\begin{aligned} y_t &= \mu + s_t + x_t \\ s_t &= \textstyle\sum_{j=1}^{4} \cos(\lambda_j t)\alpha_j + \sin(\lambda_j t)\alpha_j^* \\ (1-\phi L)x_t &= \varepsilon_t \end{aligned}$$

- fSW plus red noise model estimated via exact likelihood

$$\begin{aligned} y_t &= \mu + s_t + x_t \\ s_t &= \textstyle\sum_{j=1}^{4} \Big(\alpha_{jt} \cos(\lambda_j t) + \alpha_{jt}^* \sin(\lambda_j t)\Big) \\ (1-L)^{d_j}\alpha_{jt} &= \eta_{jt} \\ (1-L)^{d_j}\alpha_{jt}^* &= \eta_{jt}^* \\ (1-\phi L)x_t &= \varepsilon_t \end{aligned}$$

Cyclical processes: Empirical application on ice cores

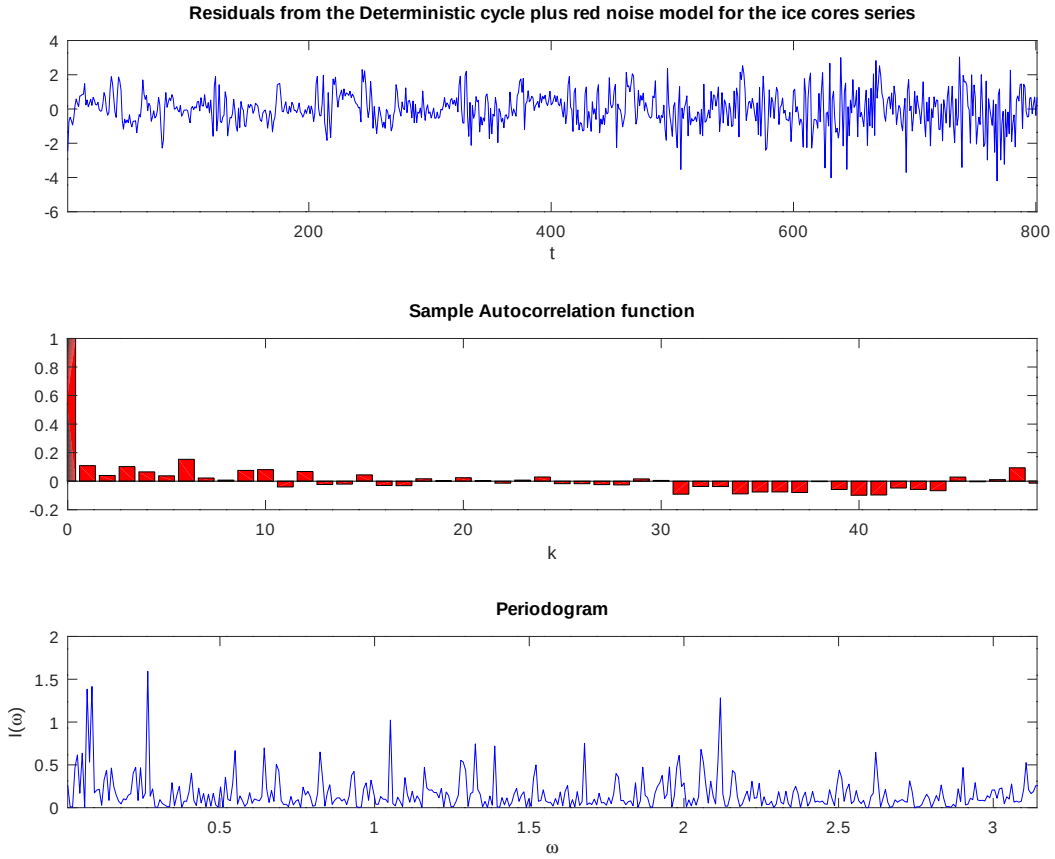

Figure: Residuals obtained from the harmonic plus red noise model: time series plot, sample autocorrelation and periodogram.

Cyclical processes: Empirical application on ice cores

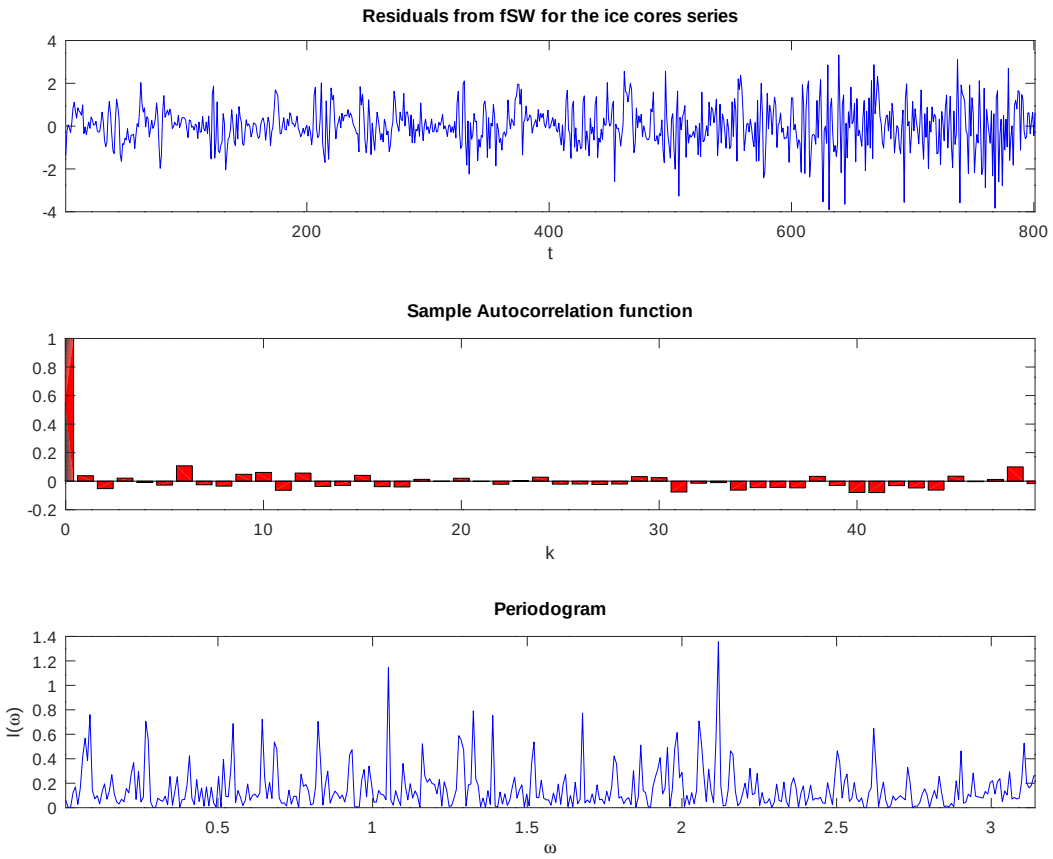

Figure: Residuals obtained from the fSW specification: time series plot, sample autocorrelation and periodogram.

Cyclical processes: Empirical application on ice cores

Harmonic model

$\hat{\mu}$	j	$\hat{\alpha}_j$	$\hat{\alpha}_j^*$	$\hat{\sigma}_\varepsilon^2$	$\hat{\phi}$	R^2
2.3350	1	0.1935	-0.045862	0.0064	0.8385	0.9026
	2	-0.1383	-0.0606			
	3	-0.0472	0.0132			
	4	-0.0111	-0.0131			

fSW model

$\hat{\mu}$	j	$\hat{d}_j$	$\hat{\sigma}_{\eta j}^2$	$\hat{\sigma}_{\alpha j}^2$	$\hat{\sigma}_\varepsilon^2$	$\hat{\phi}$	R^2
2.3317	1	0.5000	0.0000	0.0170	0.0057	0.9240	0.9029
	2	0.5000	0.0000	0.0111			
	3	0.4695	0.0006	0.0032			
	4	0.3753	0.0000	0.0000			

Table: Parameters estimates of the harmonic and fSW models for the temperature reconstruction series.

Papers References

- **[And86]** Andel, J. (1986). Long memory time series models. Kybernetika, 22 (2), 105-123.
- **[GHR01]** Giraitis, L., Hidalgo, J., Robinson, P. M., et al. (2001). Gaussian estimation of parametric spectral density with unknown pole. Annals of Statistics, 29 (4), 987-1023.
- **[GZW89]** Gray, H. L., Zhang, N.-F., and Woodward, W. A. (1989). On generalized fractional processes. Journal of time series analysis, 10 (3), 233-257.
- **[Hos81]** Hosking, J. R. M. (1981). Fractional differencing. Biometrika, 68 (1), 165-176.
- **[PM22]** Proietti, T., and Maddanu, F. (2022). Modelling cycles in climate series: The fractional sinusoidal waveform process. Journal of Econometrics.
- **[Pol05]** Pollock, S. (2005). Econometric Methods of Signal Extraction (Working Papers No. 530). Queen Mary University of London, School of Economics and Finance.
- **[VR00]** Velasco C, Robinson PM (2000) Whittle pseudo-maximum likelihood estimation for nonstationary time series. Journal of the American Statistical Association 95(452) 1229-1243.